(33 bp) of the 3′ end of *hdcA*. This organization was comparable with the well characterized *hdc* gene cluster of *Lb. buchneri* (Martine *et al.* 2005). In *P. damselae*, *hisRS* was induced at pH 4·5 and histidine excess (Fig. 7b); however, the reason for induction of *hisRS* expression under higher concentration of extracellular histidine remains unknown. One possible explanation is co-transcription of *hdcA* to *hisRS*, which is caused by the incomplete action of the transcriptional terminator of upstream genes, similar to that of the *tdc* operon of *E. faecalis* (Connil *et al.* 2002).

The *cad* operon, which encodes the lysine decarboxylation pathway, has been proposed to function in the pH homeostasis system of *Salmonella* (Foster and Hall 1990) and some of *Vibrio species* (Merrell and Camilli 2000; Rhee *et al.* 2002; Tanaka *et al.* 2008). According to the model proposed in those reports, lysine is taken up vigorously and is quickly turned over to cadaverine and CO_2, which can freely escape through the cell membrane to the atmosphere. Thus, the reaction could eliminate a large quantity of H^+ ions from the cell. It is reasonable to assume that histidine and histamine in *P. damselae* might play a role in acid survival similar to the roles of lysine and cadaverine because the transcription of *hdcT* and *hdcA* genes were significantly enhanced under acidic (pH 4·5) condition similar to elevated *cad* operon transcription under acidic condition (Merrell and Camilli 2000; Rhee *et al.* 2002; Tanaka *et al.* 2008).

In conclusion, we clarified the mechanism of histamine formation by *P. damselae*. Two enzymes were shown to be involved in producing histamine: histidine decarboxylase (*hdcA*) and putative histidine/histamine antiporter (*hdcT*), which takes histidine into the cytoplasmic space and excretes histamine from the cell. The transcripts of these genes were increased under conditions of low pH and the presence of extracellular histidine. Accumulation of histamine by *P. damselae* may confer resistance to acid stress developed through consuming intracellular protons via the decarboxylation reaction, as reported in other bacterial species (Park *et al.* 1996; Cornet *et al.* 2001; Merrell and Camilli 2002).

Acknowledgements

This work was partly supported by the Japanese Ministry of Health, Labour and Welfare (H20-011). The authors thank for Masataka Satomi, Kazuo Shiomi and Yuji Nagashima for helpful dilscussions, and also thank for Masami Ishida for conducting protein purification.

References

Altschul, S.F., Madden, T.L., Schaffer, A.A., Zhang, J., Zhang, Z., Miller, W. and Lipman, D.J. (1997) Gapped BLAST and PSI-BLAST: a new generation of protein database search programs. *Nucleic Acids Res* **25**, 3389–3402.

Arnez, J.G., Harris, D.C., Mitschler, A., Rees, B., Francklyn, C.S. and Moras, D. (1995) Crystal structure of histidyl-tRNA synthetase from *Escherichia coli* complexed with histidyl-adenylate. *EMBO J* **14**, 4143–4155.

Bearson, S., Bearson, B. and Foster, J.W. (1997) Acid stress responses in enterobacteria. *FEMS Microbiol Lett* **147**, 173–180.

Castanie-Cornet, M.P., Penfound, T.A., Smith, D., Elliott, J.F. and Foster, J.W. (1999) Control of acid resistance in *Escherichia coli*. *J Bacteriol* **181**, 3525–3535.

Connil, N., Breton, Y.L., Dousset, X., Auffray, Y., Rince, A. and Prevost, H. (2002) Identification of the *Enterococcus faecalis* tyrosine decarboxylase operon involved in tyramine production. *Appl Environ Microbiol* **68**, 3537–3544.

Cotter, P.D., Gahan, C.G. and Hill, C. (2001) A glutamate decarboxylase system protects *Listeria monocytogenes* in gastric fluid. *Mol Microbiol* **40**, 465–475.

Foster, J.W. and Hall, H.K. (1990) Adaptive acidification tolerance response of Sal*monella typhimurium*. *J Bacteriol* **172**, 771–778.

Guirard, B.M. and Snell, E.E. (1987) Purification and properties of pyridoxal-5′-phosphate-dependent histidine decarboxylases from *Klebsiella planticola* and *Enterobacter aerogenes*. *J Bacteriol* **169**, 3963–3968.

Guth, E.C. and Francklyn, C.S. (2007) Kinetic discrimination of tRNA identity by the conserved motif 2 loop of a class II aminoacyl-tRNA synthetase. *Mol Cell* **25**, 531–542.

Hirokawa, T., Boon-Chieng, S. and Mitaku, S. (1998) SOSUI: classification and secondary structure prediction system for membrane proteins. *Bioinformatics* **14**, 378–379.

Hofmann, K. and Stoffel, W. (1993) TM base – a database of membrane spanning proteins segments. *Biol Chem Hoppe-Sayler* **374**, 166.

Kamath, A.V., Vaaler, G.L. and Snell, E.E. (1991) Pyridoxal phospate-dependent histidine decarboxylase-cloning, sequencing, and expression of genes from *Klebsiella planticala* and *Enterobacter aerogenes* and properties of the overexpressed enzymes. *J Biol Chem* **266**, 9432–9437.

Kanki, M., Yoda, T., Tsukamoto, T. and Baba, E. (2007) Histidine decarboxlylases and their role in accumulation of histidine in tuna and dried saury. *Appl Environ Microbiol* **73**, 1467–1473.

Kashiwagi, K., Kuraishi, A., Tomitori, H., Igarashi, A., Nishimura, K., Shirahata, A. and Igarashi, K. (2000) Identification of the putrescine recognition site on polyamine transport protein PotE. *J Biol Chem* **275**, 36007–36012.

Kimura, B., Hokimoto, S., Takahashi, H. and Fujii, T. (2000) *Photobacterium histaminum* Okuzumi *et al.* 1994 is a later subjective synonym of *Photobacterium damselae* subsp. *damselae* (Love *et al.* 1981) Smith *et al.* 1991. *Int J Syst Evol Microbiol* **50**, 1339–1342.

Kurihara, K., Wagatsuma, Y., Fujii, T. and Okuzumi, M. (1993) Effect of culture conditions on L-histidine decar-

boxylation activity of halophilic histamine-forming bacteria. *Nippon Suisan Gakkaishi* **59**, 1401–1406.

Lin, J., Smith, M.P., Chapin, K.C., Baik, H.S., Bennett, G.N. and Foster, J.W. (1996) Mechanism of acid resistance in enrohemorrhagic *Escherichia coli*. *Appl Environ Microbiol* **62**, 3094–3100.

Martine, M.C., Fernandez, D.M., Linares, D.M. and Alvarez, M.A. (2005) Sequencing, characterization and transcriptional analysis of the histidine decarboxylase operon of *Lactobacillus buchneri*. *Microbiology* **151**, 1219–1228.

Meng, S.Y. and Bennett, G.N. (1992a) Nucleotide sequence of the *Escherichia coli cad* operon; a system for neutralization of low extracellular pH. *J Bacteriol* **174**, 2659–2669.

Meng, S.Y. and Bennett, G.N. (1992b) Regulation of the *Escherichia coli cad* operon: Location of the site required for acid induction. *J Bacteriol* **174**, 2670–2678.

Merrell, D.S. and Camilli, A. (1999) The *cadA* gene of *Vibrio cholerae* is induced during infection and plays a role in acid tolerance. *Mol Microbiol* **34**, 836–849.

Merrell, D.S. and Camilli, A. (2000) Regulation of *Vibrio cholerae* genes required for acid tolerance by a member of the "ToxR-like" family of transcriptional regulators. *J Bacteriol* **182**, 5342–5350.

Merrell, D.S. and Camilli, A. (2002) Acid tolerance of gastrointestinal pathogens. *Curr Opin Microbiol* **5**, 51–55.

Morii, H. and Kasama, K. (1995) Changes in the activity of two histidine decarboxylases from *Photobacterium phosphoreum* during growth under different oxygen tensions. *Fish Sci* **61**, 845–851.

Morii, H. and Kasama, K. (2004) Activity of two histidine decarboxylases from *Photobacterium phosphoreum* at different temperatures, pHs, and NaCl concentrations. *J Food Prot* **67**, 1736–1742.

Morii, H., Kasama, K. and Herrera-Espinoza, R. (2006) Cloning and sequencing of the histidine decarboxylase gene from *Photobacterium phosphoreum* and its functional expression in *Escherichia coli*. *J Food Prot* **69**, 1768–1776.

Murray, M.G. and Thompson, W.F. (1980) Rapid isolation of high molecular weight plant DNA. *Nucl Acids Res* **8**, 4321–4325.

Okuzumi, M., Okuda, S. and Awano, M. (1981) Isolation of psychrophilic and halophilic histamine-forming bacteria from *Scomber japonicus*. *Bull Jpn Soc Sci Fish* **47**, 1591–1598.

Okuzumi, M., Hiraishi, A., Kobayashi, T. and Fujii, T. (1994) *Photobacterium histaminum* sp. nov., a histamine-producing marine bacterium. *Int J Syst Bacteriol* **44**, 631–636.

Park, T.K., Bearson, B., Bang, S.H., Bang, I.S. and Foster, J.W. (1996) Internal pH crisis, lysine decarboxylase and the acid tolerance response of *Salmonella typhimurium*. *Mol Microbiol* **20**, 605–611.

Rhee, E.R., Rhee, J.H., Ryu, P.Y. and Choi, S.H. (2002) Identification of the *cadBA* operon from *Vibrio vulnificus* and its influence on survival to acid stress. *FEMS Microbiol Lett* **208**, 245–251.

Sambrook, J.E., Fritsch, F. and Maniatis, T.S. (1989) *Molecular Cloning: A Laboratory Manual*, 2nd edn. Cold Spring Harbor, New York: Cold Spring Harbor Laboratory.

Sanders, J.W., Leenhouts, K., Burghoorn, J., Brands, J.R., Venema, G. and Kok, J. (1998) A chloride-inducible acid resistance mechanism in *Lactococcus lactis* and its regulation. *Mol Microbiol* **27**, 299–310.

Soksawatmaekhin, W., Uemura, T., Fukiwake, N., Kashiwagi, K. and Igarashi, K. (2006) Identification of the cadaverine recognition site on the cadaverine-lysine antiporter CadB. *J Biol Chem* **281**, 29213–29220.

Tanaka, Y., Kimura, B., Takahashi, H., Watanabe, T., Obata, H., Kai, A., Morozumi, S. and Fujii, T. (2008) Lysine decarboxylase of *Vibrio parahaemolyticus*: kinetics of transcription and role in acid resistance. *J Appl Microbiol* **104**, 1283–1293.

Thompson, J.D., Higgins, D.G. and Gibson, T.J. (1994) Clustal W: improving the sensitivity of progressive multiple sequence alignment through sequence weighting, positions-specific gap penalties and weight matrix choice. *Nucleic Acids Res* **22**, 4673–4680.

Vaaler, G.L., Brash, M.A. and Snell, E.E. (1986) Pyridoxal 5′-phosphate-dependent histidine decarboxylase-nucleotide sequence of the *hdc* gene and the corresponding amino acid sequence. *J Biol Chem* **261**, 11010–11014.

Waterman, S.R. and Small, P.L.C. (1996) Identification of σ^S-dependent genes associated with the stationary-phase acid-resistance phenotype of *Shigella flexneri*. *Mol Microbiol* **21**, 925–940.

Watson, N., Dunyak, D.S., Rosely, E.L., Slonczewoski, J.L. and Olson, E.R. (1992) Identification of elements involved in transcriptional regulation of the *Escherichia coli cad* operon by external pH. *J Bacteriol* **174**, 530–540.

Yamanaka, H. and Matsumoto, M. (1989) Simultaneous determination of polyamines in red meat fishes by high performance liquid chromatography and evaluation of freshness. *J Food Hyg Soc Jpn* **30**, 396–400.

Yamane, K., Asato, J., Kawade, N., Takahashi, H., Kimura, B. and Arakawa, Y. (2004) Two cases of fatal necrotizing facilities caused by *Photobacterium damselae*. *J Clin Microbiol* **42**, 1370–1372.

Yanisch-Perron, C., Vieira, J. and Messing, J. (1985) Improved M13 phage cloning vectors and host strains: nucleotide sequences of the M13mp18 and pUC19 vectors. *Gene* **33**, 103–119.

Microbial Pathogenesis 45 (2008) 150–158

Contents lists available at ScienceDirect

Microbial Pathogenesis

journal homepage: www.elsevier.com/locate/micpath

Difference of genotypic and phenotypic characteristics and pathogenicity potential of *Photobacterium damselae* subsp. *damselae* between clinical and environmental isolates from Japan

Hajime Takahashi [a], Satoko Miya [a], Bon Kimura [a,*], Kunikazu Yamane [b], Yoshichika Arakawa [b], Tateo Fujii [a,1]

[a] Department of Food Science and Technology, Faculty of Marine Science, Tokyo University of Marine Science and Technology, 4-5-7 Konan, Minato-ku, Tokyo 108-8477, Japan
[b] Department of Bacterial Pathogenesis and Infection Control, National Institute of Infectious Diseases, Tokyo, Japan

ARTICLE INFO

Article history:
Received 8 January 2008
Received in revised form 17 April 2008
Accepted 29 April 2008
Available online 8 May 2008

Keywords:
Photobacterium
Photobacterium damselae subsp. *damselae*
Photobacterium damselae subsp. *piscicida*
Subtyping
Hemolytic activity

ABSTRACT

Photobacterium damselae subsp. *damselae* has been known as an opportunistic pathogen in fish and mammals. Human infectious cases are often very serious and occasionally fatal. We previously reportedtwo fatal cases caused by this subspecies where the patients developed multiple organ failure within 20–36 h after the onset of initial symptoms. Despite its ability to cause serious infections in humans, this subspecies has not been well studied because human infectious cases caused by this subspecies are very rare. However, this subspecies has been reported to be present in a wide range with high incidence rate in aquatic environments. Thus, we investigated the genotypic and phenotypic differences between clinical and environmental strains of *Photobacterium damselae* subsp. *damselae*. Using molecular typing methods, such as ribotyping, AFLP (Amplified Fragment Length Polymorphism), and PFGE (Pulsed-Field Gel Electrophoresis) and sequencing analysis, we determined that thetwo clinical strains were genetically similar yet distinguishable from environmental strains, but not significantly so. On the other hand, phenotypic differences were clear; moreover, mouse assay and hemolytic assay indicated strong pathogenicity of only clinical isolates. Based on these data, we concluded that there are differences in pathogenicity potential among isolates of this subspecies, and some environmental isolates have the potential to become highly pathogenic.

1. Introduction

Photobacterium damselae subsp. *damselae* was first identified as "an unnamed marine *Vibrio*" [1] when isolated and identified as the cause of a human infectious case in 1971. Upon isolation from skin ulcers of damselfish [2], this organism was named *Vibrio damsela*. Following 5S rRNA sequence analysis, it was assigned to the new genus *Listonella* [3], and following analysis of phenotypic traits, it was reassigned to the genus *Photobacterium* as *Photobacterium damselae* [4]. At the same time, during surveys of histamine-producing bacteria [5–7], an unknown species was isolated and named *Photobacterium histaminum* as a new histamine-producing species [8]. Later, this species was considered to be a synonym of *Photobacterium damselae* subsp. *damselae* based on DNA–DNA hybridization and phenotypic study [9].

Another fish pathogen, *Pasteurella piscicida* [10], was found to be closely related to this species by 16S rRNA sequence and DNA–DNA hybridization data and was reassigned to genus *Photobacterium* [11]. Accordingly, *P. damselae* was proposed to comprise two subspecies; *P. damselae* subsp. *damselae* and *P. damselae* subsp. *piscicida*, although phenotypical data clearly distinguished these two subspecies [12].

P. damselae subsp. *damselae* has been recognized as an opportunistic pathogen for a wide variety of hosts such as a broad range of fish [13–16] and mammals [17], including humans [1]. In human cases, once infected, most patients become critical and many fatalities occur despite antibiotic treatments at the early infection stage [18–24]. Although some human infectious cases have occurred in people with notable medical histories [18,22,23], people with no underlying illnesses commonly suffer serious damages [1,23].

Previous reports on surveys of histamine-producing bacteria showed an occurrence rate of this bacterium of $1–10^3$ CFU l^{-1} in seawater around Tokyo, Japan for this species [25]. In other surveys, this species has been isolated from a wide range of environments such as estuarine and marine water, sediment, and healthy aquatic animals [26,27]. In Spain, a survey of five different fish farms

* Corresponding author. Tel./fax: +81 3 5463 0603.
E-mail address: kimubo@kaiyodai.ac.jp (B. Kimura).
[1] Present address: Yamawaki Gakuen Junior College, 4-10-36 Akasaka, Minato, Tokyo 107-8371, Japan.

0882-4010/$ – see front matter © 2008 Elsevier Ltd. All rights reserved.
doi:10.1016/j.micpath.2008.04.008

showed detection rates of 10% in asymptomatic gilthead sea bream and 6% in sea bass with rates that were even higher in warm months [13]. Furthermore, a number of marine animal diseases associated with this organism have been reported around the world [16]. However, only a few human infectious cases linked to either consumption of contaminated seafood [22] or wound infections have been reported so far. Given the wide distribution and high occurrence rate of this bacterium, the number of human infectious cases is relatively low. Moreover, different levels of symptom development have been observed among infected people; that is, some infected people die within a few days of infection despite early intervention, while some make full recoveries. This suggests that there are different levels of virulence potential for humans within this species with a high prevalence of members in the marine environment that are either not pathogenic or weakly pathogenic toward humans, while only a portion of strains possess strong pathogenicity. In fact, the virulence potential of this organism for fish has been reported to be species-specific [14,28].

In our previous study [23], we encounteredtwo fatal cases of wound infections caused by *P. damselae* subsp. *damselae*. The patients developed multiple organ failure within 20–36 h after the onset of initial symptoms. While one victim had a history of diabetes mellitus, the other had no remarkable medical history. Using these deadly clinical isolates of this species and other isolates from the environment, we investigated the genotypic and phenotypic differences between clinical and environmental isolates, as well as their pathogenicity for mice to evaluate pathogenic potential of *P.damselae* subsp. *damselae* isolates for humans.

2. Results

2.1. Phylogenetic analysis with gyrB, toxR and ompU genes

An UPGMA dendrogram was constructed for 15 isolates (13 environmental andtwo clinical) of *P. damselae* subsp. *damselae* and 4 of *P. damselae* subsp. *piscicida* based on composite data of partial sequences ofthree housekeeping genes (Fig. 1): *gyrB*, *toxR* and *ompU*. Thesethree genes were selected because they have been reported to be suitable for phylogenetic studies of *Vibrio* species, which are evolutionally close to *Photobacterium* species [29–31]. Amplification of *toxR* and *ompU* failed for other *Photobacterium* strains despite trials with different primers and amplification conditions. While *P. damselae* subsp. *piscicida* strains showed 100% identical sequences for allthree loci, those of *P. damselae* subsp. *damselae* strains were diverse, having nine distinct sequences among 15 isolates at each locus with similarity values of >97.8%, >94.1%, and >62.8% in *gyrB*, *toxR*, and *ompU*, respectively. Althoughtwo clinical *P. damselae* subsp. *damselae* strains showed distinct sequences for allthree loci, they had high similarity values in *gyrB* and *ompU* of 99.0% and 99.1%, respectively. Moreover, deduced amino acid sequences were 100% identical in thesetwo isolates for *gyrB* whereasthree and only one amino acid residues were different in *toxR* and *ompU*, respectively. This close relationship between thesetwo clinical isolates is shown in the dendrogram (Fig. 1). These clinical isolates, together with one environmental isolate, clustered together and distinctly from other environmental isolates and *P. damselae* subsp. *piscicida* isolates.

Similarity values between *P. damselae* subsp. *piscicida* and *P. damselae* subsp. *damselae* were >88.0%, indicating their close relationship.

2.2. Ribotyping

Using the automated RiboPrinter microbial characterization system as a typing system for members of this genus, all the *Photobacterium damselae* subsp. *damselae* isolates were shown to share a similar ribotype with similarity values of >95.5% and sharing one visible strong band (Fig. 2). In particular,two clinical isolates, PDA1 and PDA2, showed significant similarity (99.2%). All the *P. damselae* subsp. *piscicida* formed a single cluster, which is closer to *P. damselae* subsp. *damselae* than to other *Photobacterium* spp.

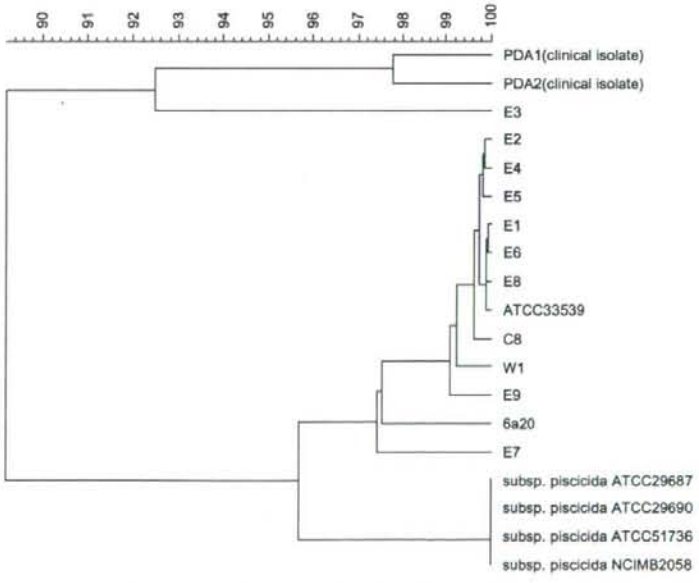

Fig. 1. UPGMA dendrogram constructed based on composite sequence data of *gyrB*, *toxR*, and *ompU* genes using Bionumerics software. Similarity percentages are shown above the dendrogram.

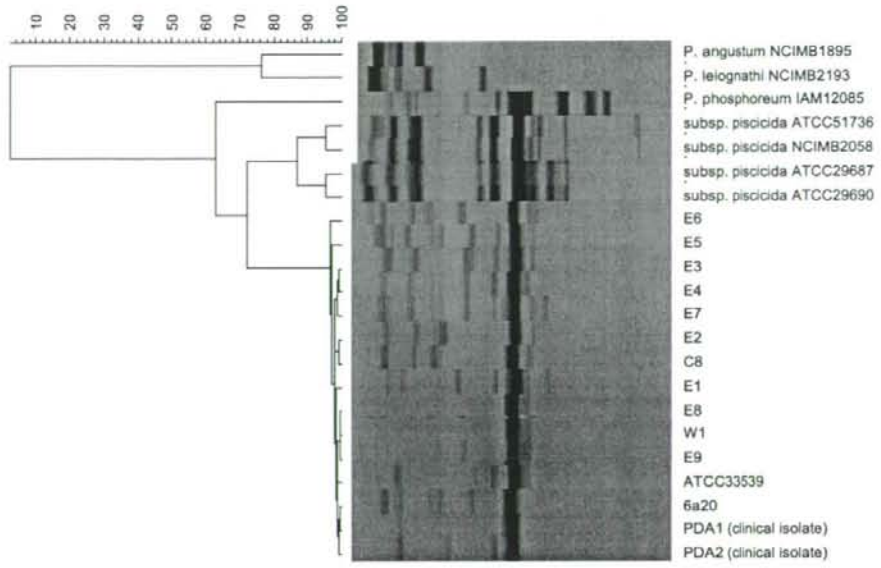

Fig. 2. UPGMA dendrogram constructed based on ribotyping. Dendrogram was constructed using Bionumerics software based on the image obtained by automated RiboPrinter system. Similarity percentages are shown above the dendrogram.

2.3. AFLP analysis

The AFLP profiles clearly separated *P. damselae* from other *Photobacterium* spp. in the dendrogram (Fig. 3). *P. damselae* subsp. *damselae* and *P. damselae* subsp. *piscicida* clustered together, with the constituents of each subspecies grouped with each other. In this dendrogram, thetwo clinical isolates of *P. damselae* subsp. *damselae*, PDA1 and PDA2, closely clustered with a similarity value of 89.4. The other three *Photobacterium* spp., *P. angustum*, *P. leiognathi*, and *P. phosphoreum*, were clearly outgrouped, indicating the close relationship of *P. damselae* subsp. *piscicida* and *P. damselae* subsp. *damselae* as subspecies.

2.4. PFGE

The PFGE banding patterns were very heterogeneous among the analyzed isolates without showing any specific pattern in common (Fig. 4). P. *damselae*, including both subspecies *damselae* and

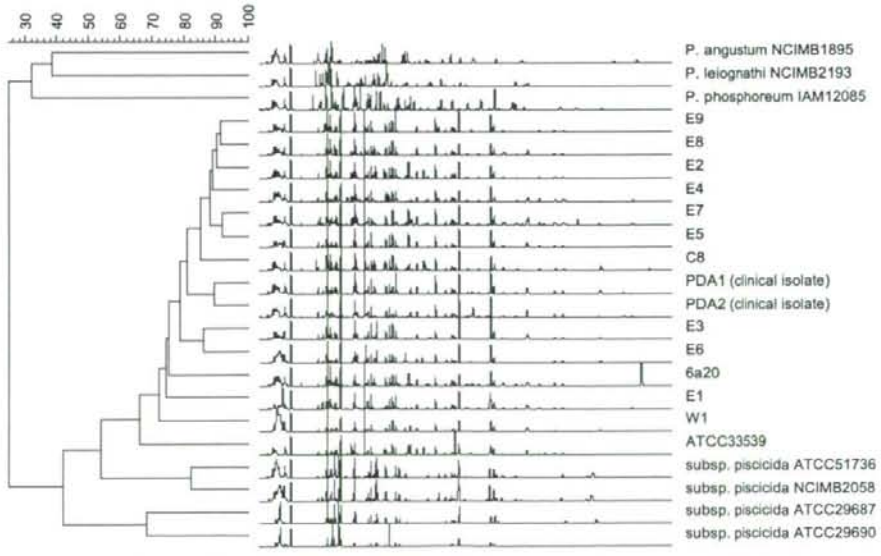

Fig. 3. UPGMA dendrogram constructed based on AFLP analysis. Dendrogram was constructed using Bionumerics software based on the densitometric values obtained by GeneScan Analysis software following electrophoresis. Similarity percentages are shown above the dendrogram.

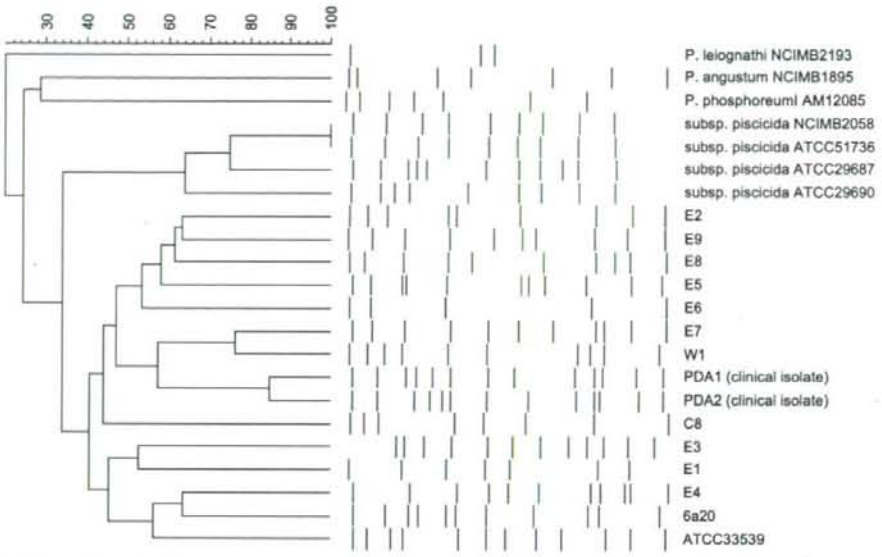

Fig. 4. UPGMA dendrogram constructed using Bionumerics software based on the electrophoretic image in the PFGE analysis. Similarity percentages are shown above the dendrogram.

piscicida, formed a single, large cluster, positioned distinctly from other *Photobacterium* spp. Within this large cluster, the two subspecies formed two different small clusters. Whereas very heterogeneous pattern was shown among *P. damselae* subsp. *damselae* isolates, thetwo clinical isolates of *P. damselae* subsp. *damselae*, PDA1 and PDA2, were positioned relatively closely to each other with a similarity value of 84.6.

2.5. Biochemical properties

A dendrogram based on biochemical property profiles (Table 3) was constructed for *Photobacterium* strains (Fig. 5). Whereas *P. damselae* subsp. *damselae* environmental strains showed highly similar profiles (similarity values of ≥82.8),two clinical strains of this species, PDA1 and PDA2, showed profiles distinct from these environmental strains. This distinction was reflected in the formation of a cluster comprised of thetwo clinical strains separate from that of the environmental strains in the dendrogram. The four isolates of *P. damselae* subsp. *piscicida* formed a single cluster, which is distant from the cluster of *P. damselae* subsp. *damselae* isolates (Fig. 5). This placement indicates the high degree of differences in the phenotypic characteristics between these subspecies (Table 1).

2.6. Hemolytic activities

The hemolytic activities of *P. damselae* subsp. *damselae* were roughly divided into two groups based on hemolytic halo diameter (Table 1): large halo, 7–8 mm and small halo, 2–3 mm. Thetwo clinical isolates of this species, PDA1 and PDA2, along with four environmental strains, showed large haloes, whereas the majority of environmental strains (9/13) showed small ones. The other *Photobacterium* strains, including *P. damselae* subsp. *piscicida* strains, showed no hemolytic activity to sheep erythrocytes.

2.7. Mouse virulence

The LD_{50} values of all the tested *P. damselae* subsp. *damselae* isolates ranged from 2.8×10^8 to 1.5×10^6 (Table 1). The lowest LD_{50} values, 2.4×10^6 and 1.5×10^6, were recorded for PDA1 and PDA2, respectively, indicating their strong pathogenicity for mice. These were 1–2 orders of magnitude lower than those of environmental strains where LD_{50} values ranged from 1.0×10^7 to 2.8×10^8. For other *Photobacterium* spp. isolates, including those of *P. damselae* subsp. *piscicida*, no mortality of mice was observed even for inoculation of $\geq 10^8$ CFU.

Animal mortality was monitored for 7 days, but mice either died within 24 h of inoculation or remained alive throughout the 7-day test period.

3. Discussion

We have previously encountered two cases of human infections of *Photobacterium damselae* subsp. *damselae* [23]. Both patients died, which is shocking since this bacterium is ubiquitous in aquatic environments and is often isolated from fish [32]. The known incidence of these bacteria raises the question of whether environmental isolates are as pathogenic as clinical isolates—very important information for preventing further infectious cases.

Using genomic typing methods of sequencing analysis, ribotyping, AFLP and PFGE, genomic diversity among *P. damselae* subsp. *damselae* isolates was characterized. Among the very diverse profiles,two clinical isolates, PDA1 and PDA2, had relatively similar genotypes, as shown in the dendrograms (Figs. 1–4). Although the venues of infection caused by these two isolates were distant, Okinawa prefecture and Okayama prefecture in Japan, it is possible that they were recently derived from a common progenitor. However, no visualized band or banding patterns or sequences specific to only clinical isolates were observed. The placement of clinical isolates among environmental isolates in the dendrograms demonstrates that although clinical isolates are closely related genetically, they are not clearly distinguishable from environmental isolates. Although they were clearly separated from most of the environmental strains in sequence analysis, they were still clustered together with one environmental isolate (Fig. 1).

Compared to these genotypic characteristics, the phenotypic typing showed distinct profiles for clinical isolates of *P. damselae*

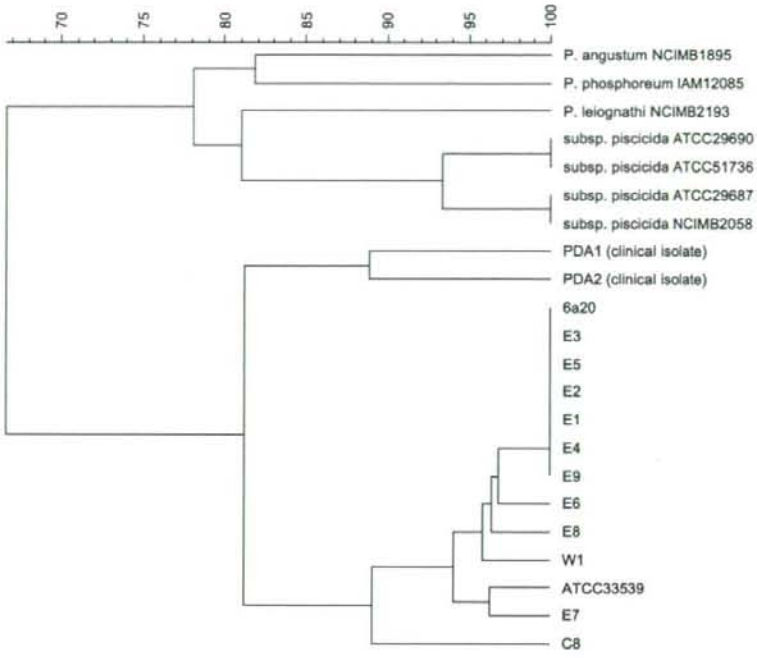

Fig. 5. UPGMA dendrogram constructed based on biochemical properties of the isolates. The obtained data using API 20E and API 50CHE were transferred into Bionumerics software to construct the dendrogram. Similarity percentages are shown above the dendrogram.

subsp. *damselae*. In a dendrogram constructed based on biochemical property profiles (Fig. 5), clinical isolates not only showed a relatively close relatedness to each other as shown in the dendrograms for the genomic typing, but they also formed a cluster clearly distinct from that of environmental isolates. This is impressive because such a clear distinction was not observed in analysis of genotypes. The clinical isolates also showed distinct characteristics in pathogenicity profiles for mice compared to environmental isolates (Table 1). One explanation of this inconsistency between the results based on genotypic and phenotypic data is that divergence of clinical strains from environmental ones is a recent event and these phenotypic differences are still so small that they are not detected by whole genome typing techniques such as PFGE and AFLP. Ribotyping showed even smaller differences between clinical and environmental isolates because rDNA is highly conserved and evolves slowly [33,34]. On the other hand, sequencing analysis of the *gyrB*, *toxR*, and *ompU* genes showed larger differences between clinical and environmental isolates. Previously, the *gyrB* gene was proposed as a suitable phylogenetic marker for the classification of bacteria because the molecular evolutionary rate of the *gyrB* gene is higher than that of 16S rDNA [34]. The same is probably true for *toxR* and *ompU* genes, as is shown in the dendrogram (Fig. 5).

Table 1
Genus *Photobacterium* strains used in this study and their pathogenic characteristics

Strain	Source	Hemolytic activity[a]	LD_{50} (CFU/mouse)
P. damselae subsp. *damselae*			
PDA1	Clinical	L	2.4×10^6
PDA2	Clinical	L	1.5×10^6
ATCC 33539	Damselfish	S	8.7×10^7
E1	Horse mackerel	S	2.8×10^8
E2	Horse mackerel	S	6.4×10^7
E3	Horse mackerel	L	2.0×10^7
E4	Horse mackerel	S	9.3×10^7
E5	Horse mackerel	S	1.9×10^8
E6	Horse mackerel	S	1.8×10^8
E7	Horse mackerel	L	1.2×10^7
6a20	Horse mackerel	S	9.9×10^7
E8	Sardine	L	1.0×10^7
E9	Sardine	S	2.7×10^8
C8	Labracoglossid fish	S	2.5×10^8
W1	Sea water	L	1.6×10^8
P. damselae subsp. *piscicida*			
ATCC 29687	Yellowtail	ND[b]	ND[c]
ATCC 29690	Yellowtail	ND	ND
ATCC 51736	Yellowtail	ND	ND
NCIMB 2058	Yellowtail	ND	ND
P. angustum NCIMB 1895	Seawater	ND	ND
P. leiognathi NCIMB 2193	Teleostean fish	ND	ND
P. phosphoreum IAM 12085	Cock rhynchus	ND	ND

[a] L, large hemolytic halo; S, small hemolytic halo.
[b] ND, hemolytic activity was not detected.
[c] ND, LD_{50} was greater than the maximum dose used.

Pathogenicity of *P. damselae* subsp. *damselae* isolates for mice and hemolytic activity were positively correlated (Table 1); except for strain W1, the remaining five strains with large hemolytic haloes ranked among the five most pathogenic strains for mice. This correlation was previously demonstrated for LD_{50} values for mice and hemolytic activities for mouse erythrocytes [35]. Although this and another report [36] showed much weaker sensitivity of sheep erythrocytes to *Photobacterium damselae* subsp. *damselae* compared to mouse and rat erythrocytes, we demonstrated a correlation between hemolytic activity for sheep erythrocytes and pathogenicity for mice. Other researchers have categorized human clinical isolates into highly virulent strain groups because of their relatively low LD_{50} values for mice and fish

[28,37] and their strong hemolytic activity [37]. Likewise, the two human clinical isolates used in our study are expected to be categorized into highly pathogenic group based on their LD_{50} values and hemolytic activity. While thetwo human clinical isolates in our study were shown to be highly pathogenic, levels of pathogenicity among environmental isolates of *P. damselae* subsp. *damselae* were variable. Strongly hemolytic isolates, such as E3, E7, E8, had stronger pathogenicity for mice compared to other environmental isolates (including strongly hemolytic strain W1). Although these isolates did not specifically group together in genomic typing (Figs. 1–4), these could be categorized as moderately pathogenic isolates. We also analyzed the plasmid contents of *P. damselae* subsp. *damselae* isolates used in this study. Plasmid contents were observed in all of the strongly hemolytic isolates, but not in weakly hemolytic ones (except ATCC 33539, which was weakly hemolytic but had a plasmid) (data not shown), indicating a contribution of plasmid contents to hemolytic activities. This needs further analysis for determination.

Our genotypic and phenotypic analyses of *P. damselae* subsp. *damselae* isolates and four *P. damselae* subsp. *piscicida* isolates show that thesetwo subspecies are closely related based on genotypes but distinct in phenotypic characteristics (Figs. 1–5), consistent with previous reports. Previously Gauthier et al. [11] proposed *P. damselae* subsp. *piscicida* as a subspecies of *P. damselae* based on its genetic relatedness to *P. damselae* subsp. *damselae*, and later Thyssen et al. [38] concurred based on AFLP and DNA–DNA hybridization analyses despite the observation of phenotypical characteristics distinct from those of *P. damselae* subsp. *damselae* [12]. In our study, *P. damselae* subsp. *piscicida* had no hemolytic activity and no pathogenicity for mice (Table 1), showing characteristics different from those of *P. damselae* subsp. *damselae*. Because of this phenotypic and genotypic inconsistency, the taxonomic position of this species within *Photobacterium* spp. is still debatable.

In this study, analysis of subspecies heterogeneity revealed that genetically similar clinical and environmental isolates had substantial phenotypic variation that alters the pathogenic potential. Overall, thetwo clinical isolates of *P. damselae* subsp. *damselae* isolated from two temporally- and spatially-separated different areas were genetically close to each other and strongly pathogenic. Some environmental strains showed moderately strong pathogenicity. This leaves two possible pathways for future infections. One is that a strongly pathogenic isolate multiplies and proliferates over a wide geographic range, as PDA1 and PDA2 might have done. Another is that moderately pathogenic strains turn into strongly pathogenic strains. In either case, sporadic or even epidemic cases can happen, and it can be a big issue since this bacterium is known to have a potential to cause fatal disease. However, our analysis of pathogenic strains was limited totwo clinical isolates, both of which were isolated in Japan. It may be necessary to analyze a larger number of geographically diverse isolates in order to produce more convincing results. Also, factors affecting the pathogenic potential of *P. damselae* subsp. *damselae* isolates, such as ability to colonize inside hosts, require further investigation.

4. Materials and methods

4.1. Bacterial strains

The 22 bacterial strains used in this study are summarized in Table 1. One strain of *Photobacterium damselae* subsp. *damselae* and the other *Photobacterium* spp. strains were obtained from the following collections: American Type Culture Collection (ATCC; Manassas, VA, USA), the Institute of Molecular and Cellular Biosciences (IAM; Tokyo, Japan), and National Collections of Industrial, Food and Marine Bacteria Japan (NCIMB; Shizuoka, Japan). *P. damselae* subsp. *damselae* clinical strains were obtained as described previously [23], and environmental isolates were collected from different types of fish and seawater in Japan between 2002 and 2003. Environmental isolates were screened for histamine forming activity as described previously [39]. Briefly, fresh skinned fish fillets were obtained from various grocery stores in and around Tokyo, Japan. Muscle tissue (5 g) was aseptically removed from each sample and placed in 45 ml histidine broth (pH 5.0) containing (per liter) 10 g Bactopepton (Difco Laboratories, Detroit, MI, USA), 3 g yeast extract (Difco), 5 g glucose and 5 g L-histidine (Wako Pure Chemical Industries, Osaka, Japan) in 50% artificial sea water (ASW) [4]. The homogenate of the mixture was incubated at 25 °C for 24 h and each culture was assayed for the presence of histamine using paper chromatography as described previously [40]. Briefly, 5 µl of the culture was applied to Advantec filter paper (No. 51B, 40 cm × 40 cm) (Toyo Roshi, Tokyo, Japan), and a solvent consisting of butanol and 10% NH_4OH (1:1) was applied following by spraying Pauly's diazo reagent. Samples identified as being positive for histamine were incubated on Niven's agar [41] supplemented with 50% ASW and the colonies light purple in color were identified using the API ID 32E (bioMérieux, Marcy l'Etoile, France) following the manufacturer's instructions.

Isolates identification was further confirmed by amplifying and sequencing approximately 400–450 bp of 16S ribosomal DNA (rDNA) (position 50–450 or –500 [*Escherichia coli* numbering]). Amplification was conducted using universal primers 27F and 1492R [42], and the amplification products were purified for use in direct sequencing with primer 27F. Resulting sequences were then used to search the DNA DataBank of Japan (DDBJ; Shizuoka, Japan) (http://www.ddbj.nig.ac.jp) by the BLAST 2.0 algorithm to confirm identification.

Isolated strains were stored in a microbank (Aska Diagnostics, Tokyo, Japan) at −80 °C. One day prior to each experiment, the frozen culture was transferred into enrichment broth for use.

4.2. DNA extraction

Bacterial strains were cultured in enriched brain heart infusion broth (BHI; Becton Dickinson, Sparks, MD) supplemented with 50% ASW (BHI-1) and DNA was extracted using the phenol–chloroform and ethanol precipitation [43]. Briefly, a 1-ml sample of enriched culture was centrifuged at 10,000 × *g* for 10 min, the bacterial cells were incubated in 567 µl of Tris–EDTA buffer containing lysozyme (2 mg ml^{-1}) for 1 h at 37 °C, and cells were lysed by adding 30 µl of 10% (w/v) sodium dodecyl sulfate and 3 µl of 20 mg proteinase K μl^{-1} followed by incubation for 1 h at 37 °C. Next, 100 µl of 5 M NaCl was added, and DNA was extracted with chloroform–isoamyl alcohol (24:1) followed by phenol–chloroform–isoamyl alcohol (25:24:1). DNA was then precipitated with isopropanol, washed with 70% ethanol, and dried. Purified DNA samples were resuspended in Tris-EDTA buffer and used as DNA templates.

4.3. Sequencing analysis of gyrB, toxR and ompU genes

All *Photobacterium damselae* isolates, including those of subsp. *damselae* and subsp. *piscicida*, were sequenced for *gyrB, toxR and ompU* genes. PCR primers used and the amplification conditions of *gyrB, toxR and ompU* genes are shown in Table 2. Primers used to amplify the *gyrB* gene were from a previous study [34], and all other primers were designed in this study (Table 2). PCR amplification was performed in 100-µl reaction mixtures: 10 mM Tris–HCl (pH 8.3), 50 mM KCl, 1.5 mM $MgCl_2$, 20 pmol of each primer, 0.2 mM each of the four dNTPs, 0.5 U Taq DNA polymerase (Takara, Shiga, Japan), and template DNA (50 ng). Amplifications were carried out with an initial denaturation at 94 °C for 5 min, a final extension at 72 °C for 4 min, and thermal cycle programs modified to each amplification target (Table 2) in a GeneAmp PCR 9700 thermal

Table 2
Amplification and sequence primers and PCR conditions

Gene	Primer		Reference	PCR conditions	
	Primer name[a]	Sequence		No. of cycles	Cycle steps
gyrB	UP-1	CAYGCXGGXGGXAARTTYGA	Yamamoto et al. (1995)	30	94 °C for 30 s, 60 °C for 1 min, 72 °C for 1.5 min
	UP-2r	CCRTCXACRTCXGCRTCXGTCAT	Yamamoto et al. (1995)		
	GYR-1f*	TAGHGCRACTCCHTACAA	This study		
	GYR-1r*	CTRGGATTYAAGAGWTCGGT	This study		
	GYR-2f*	ACCGAWCTCTTRAATCCYAG	This study		
	GYR-2r*	TTGTADGGAGTYGCDCTA	This study		
toxR	TOX-f	TTAAAGATCCAACCAAGTCTC	This study	30	94 °C for 30 s, 52 °C for 30 s, 72 °C for 30 s
	TOX-r	GTYGAAATKAGGYTCTGCCA	This study		
ompU	OMP-f	GGTATGATCACTGACTTTACCGA	This study	35	94 °C for 30 s, 55 °C for 1 min, 72 °C for 1 min
	OMP-r	TAACCTGCGTAAGTACGGAA	This study		

[a] Primers marked with * were used only for sequencing. Other primers were used for both amplification and sequencing.

cycler (Applied Biosystems, Foster City, CA, USA). PCR products (10 μl) were separated by 1% agarose gel electrophoresis at 100 V in 1× TAE buffer (pH 8.3; 40 mM Tris, 20 mM acetate, and 1 mM EDTA) along with suitable molecular markers (100-base-pair ladder, Bio-Rad, Hercules, CA, USA), and visualized with ethidium bromide under UV (245 nm) to confirm that amplification products of the expected size were produced. The amplified fragments were treated with polyethylene glycol (PEG), cooled on ice for 1 h, and pelleted by centrifugation at 15,000 × *g* for 20 min. The pellet was washed with 70% ethanol, dried, and dissolved in TE buffer. Purified DNA fragments were sequenced using an ABI 310 DNA sequencer with BigDye terminator v.3.1 cycle sequencing kits (Applied Biosystems). PCR amplification primers along with four additional primers designed for sequencing the *gyrB* gene (Table 2) were used for sequencing the partial *gyrB*, *toxR*, and *ompU* genes with varied lengths of 539 bp, 376–391 bp, and 447–474 bp, respectively. Obtained sequences were deposited in the DNA Data Bank of Japan (DDBJ; National Institute of Genetics, Shizuoka, Japan) under accession numbers AB364522 through AB364578. A preparation of composite Unweighted Pair Group Method with Arithmetic mean (UPGMA) dendrogram with average linkage (Fig. 1) and calculations of similarity values were conducted using the obtained sequences in Bionumerics v.4.0 software (Applied Maths, Sint-Martens-Latem, Belgium).

4.4. Ribotyping

All *Photobacterium* strains used in this study were characterized by automated ribotyping using a RiboPrinter microbial characterization system (Dupont Qualicon, Wilmington, DE) following the manufacturer's instructions. Briefly, isolates were streaked onto Trypticase soy agar plates (Becton Dickinson) supplemented with 50% ASW (TSA-1), then appropriate amount of colonies was used for the analysis. Following automated cell lysis, digestion of DNA with EcoRI, electrophoresis, transfer of fragments, hybridization with an *E. coli* rRNA operon probe and detection of hybridized bands with chemiluminescence, the resulting ribotypes were used to construct a dendrogram based on the Pearson product-moment correlation coefficient and UPGMA using BioNumerics software (Fig. 2).

4.5. Amplified Fragment Length Polymorphism (AFLP) analysis

All *Photobacterium* isolates used in this study were subjected to AFLP Microbial Fingerprinting Kit (Applied Biosystems). Briefly,

Table 3
Biochemical properties of *Photobacterium* spp.

Biochemical test[a]	Positive reactions (no. of isolates)					
	P. damselae subsp. *damselae*		*P. damselae* subsp. piscicida (*n* = 4)	*P. angustum* (*n* = 1)	*P. leiognathi* (*n* = 1)	*P. phosphoreum* (*n* = 1)
	Clinical strains (*n* = 2)	Environmental strains (*n* = 13)				
β-Galactosidase	–	2	–	–	–	–
Arginine dihydrolase	1	13	2	–	1	1
Lysine decarboxylase	–	–	–	–	–	1
Urease	2	13	–	–	–	–
Gelatinase	2	1	–	–	–	–
NO_3 to NO_2	2	12	–	–	1	–
Fermentation of:						
Glycerol	2	13	–	–	1	–
D-Xylose	–	–	–	–	1	–
α-Methyl-D-glucoside	2	–	–	–	–	–
Esculin	1	–	–	–	–	–
Salicin	1	–	–	–	–	–
Celliobiose	2	13	–	–	–	–
Maltose	2	13	–	1	–	1
Trehalose	2	11	–	–	–	–
Starch	–	11	–	–	–	–
Glycogen	–	1	–	–	–	–
Gentiobiose	1	–	–	–	–	–
D-Turanose	2	–	–	–	–	–
Gluconate	–	–	–	1	1	1
Sucrose	–	–	–	1	–	–

[a] Biochemical tests of ornithine decarboxylase, H_2S production, tryptophan deaminase, tryptophanase, utilization of citrate, and fermentation of D-mannitol, inositol, D-sorbitol, L-rhaminose, L-arabinose, erythritol, D-arabinose, L-arabinose, L-xylose, adonitol, β-methyl-D-xyloside, sorbose, dulcitol, α-methyl-D-mannoside, arbutin, lactose, inulin, melezitose, raffinose, xylitol, D-lyxose, D-tagatose, D-fucose, L-fucose, D-arabitol, L-arabitol, 2-keto-gluconate, 5-keto-gluconate, amygdalin, and melibiose showed negative results for all Photobacterium strains tested. Voges–Proskauer test and fermentation of ribose, galactose, fructose, mannose, *N*-acetyl glucosamine, and glucose showed positive results for all *Photobacterium* strains tested.

10 ng of extracted bacterial DNA was digested with 2.5 U of MseI and 5 U of EcoRI restriction enzymes and was subsequently ligated to MseI and EcoRI restriction site-specific adapters by overnight incubation at room temperature. Preselective PCR was carried out with a GeneAmp 9700 thermal cycler in 20-μl reaction mixtures containing 4 μl of the restriction ligation mixture, 0.5 μl of preselective MseI primer of manufacturer-defined concentration, 0.5 μl of preselective EcoRI primer of manufacturer-defined concentration, and 15 μl of AFLP Amplification Core Mix. Amplification products were diluted 20:1 with $TE_{0.1}$ buffer (20 mM Tris–HCl, 0.1 mM EDTA, pH 8.0) and used as template (1.5 μl) in selective PCR, carried out with a reaction volume of 10 μl mixture and the reaction conditions described above with MseI-selective primer and fluorescently labeled EcoRI-selective primer. MseI and EcoRI primers containing adjacent nucleotide A, C, G or T were tested for optimization. Aliquots (0.5 μl) of selective amplification products were mixed with 25 μl of deionized formamide and 1 μl of GeneScan-500 [ROX] size standard (Applied Biosystems), denatured at 95 °C for 3 min and immediately cooled on ice. AFLP capillary electrophoresis was performed on an ABI Prism 310 Genetic Analyzer (Applied Biosystems). After electrophoresis, the AFLP patterns were automatically analyzed using GeneScan Analysis software (Applied Biosystems). Densitometric values were transferred to the BioNumerics software and cluster analysis was performed using Pearson coefficients and the UPGMA clustering algorithm (Fig. 3).

4.6. Pulsed-field gel electrophoresis (PFGE)

Of eight restriction endonucleases tested under numerous electrophoretic conditions, only SfiI used under the condition described below generated fragment patterns appropriate for differentiating *Photobacterium* strains. Bacterial plugs were prepared using the Bio-Rad CHEF Bacterial Genomic DNA Plug Kit (Bio-Rad) following the manufacturer's instructions with a minor modification. Briefly, isolated strains were cultured in BHI-1 at 30 °C until reaching OD_{600} of 0.8. Subsamples (1 ml) were incubated with chloramphenicol at a final concentration of 180 μg ml^{-1} for another 1 h. The suspensions were centrifuged at 10,000 × *g* for 3 min at 4 °C. Pellets were resuspended in Suspension Buffer to which 2% CleanCut agarose was added to achieve a final concentration of 1%. The cell–agarose mixture was transferred to disposable plug molds and maintained at 4 °C for 10 min for the mixture to solidify. The plugs were pushed out into wells containing 12 μl of lysozyme stock and 300 μl of lysozyme buffer in 24-well polystyrene plates. After incubating at 37 °C for 2 h with gentle agitation, the lysozyme solution was removed. The plugs were washed with sterile water, and incubated overnight at 50 °C with 300 μl of Proteinase K reaction buffer and 12 μl of Proteinase K stock. The plugs were washed four times in 1× Wash Buffer, with each wash lasting 1 h and 1 mM phenylmethanesulfonylfluoride replacing 1× Wash Buffer in the third wash. The buffer was aspirated and 30 U of SfiI with the appropriate amount of buffer was added to each plug. The plugs were incubated in the presence of this enzyme for 17 h, cut into appropriate sizes, loaded into the wells of the agarose gel (1% Seakem Gold Agarose, Cambrex, Rockland, ME, USA), and electrophoresed for 18 h in 0.5 × TBE buffer at 14 °C with an applied voltage of 6 V with Bio-Rad CHEF-DR II system. Initial time of 5 s and final time of 50 s were selected. DNA bands were visualized under UV light after ethidium bromide staining. A dendrogram was constructed using BioNumerics software based on Dice coefficient and UPGMA parameters (Fig. 4).

4.7. Biochemical properties

Biochemical properties of the *Photobacterium* isolates were characterized using API commercial test kit (Table 1): API 20E and API 50CHE (bioMérieux). The tests were performed following the manufacturer's instructions with modifications in the suspension broth, length and temperature of incubation. Briefly, colonies grown on BHI-1 agar plates for each isolate were suspended in media specific to each test, to which NaCl was supplemented to a final concentration of 1.5% (w/v). Bacterial suspensions were inoculated into strips for each test following manufacturer's instructions and incubated at 26 °C for 72 h according to Thyssen et al. (1998). Every questionable test result was repeated twice or more. A dendrogram was constructed using BioNumerics software based on Dice coefficient and UPGMA (Fig. 5).

4.8. Hemolytic activity assay

Hemolytic activity was assayed on sheep blood agar for all *Photobacterium* isolates used in this study. Sheep blood was selected because it has been shown to have the same level of susceptibility to *P. damselae* subsp. *damselae* as human blood does [35,36]. Each strain was grown in TSB-1 to early log phase. The culture was streaked onto TSA-1 plates, allowed to dry for 10 min, then overlaid with 6 ml of soft TSA-1 supplemented with 5% sheep blood, which had been melted and kept warm. After solidification, the plates were incubated at 30 °C for 24 h, and then the diameter of hemolytic halo was measured in millimeters (Table 1). Experiments were done in triplicate.

4.9. Mouse virulence

Male ddY 4-week-old mice (Sankyo Labo Service, Tokyo, Japan) each weighing 20–22 g were used to assay pathogenicity. Mice were allowed free access to water and chow diet throughout the experimental period. Each bacterial strain was cultured to mid-log growth phase in BHI-1 broth, and diluted 10-fold to produce cell suspensions in the range of 10^5–10^8 CFU 0.1 ml^{-1} in phosphate-buffered saline. Mice were divided into groups of five each and injected intraperitoneally with 0.1 ml of either sterile PBS (control) or cell suspensions at each concentration. Bacterial counts of the inocula were confirmed by plating serially diluted cultures onto BHI-1 agar in duplicate using a spiral plater (IUL S.A., Barcelona, Spain). Mortality was observed for 7 days and LD_{50} was calculated for each strain using the method of Reed and Muench [44].

Acknowledgements

We thank Chika Saito and Chikako Kamimura for technical support.This work was partly supported by Japanese Ministry of Health, Labour and Welfare (H20-011).

References

[1] Morris Jr JG, Wilson R, Hollis DG, Weaver RE, Miller HG, Tacket CO, et al. Illness caused by *Vibrio damselae* and Vibrio hollisae. Lancet 1982;i:1291–7.
[2] Love M, Teebken-Fisher D, Hose JE, Farmer III JJ, Hickman FW, Fanning FW. *Vibrio damselae*, marine bacterium causes skin ulcers on the damselfish *Chromis punctipinnis*. Science 1981;214:1139–40.
[3] MacDonell MT, Colwell RR. Phylogeny of the *Vibrionaceae*, and recommendation for two new genera, *Listonella* and *Shewanella*. Syst Appl Microbiol 1985; 6:171–82.
[4] Smith SK, Sutton DC, Fuerst JA, Reichelt JL. Evaluation of the genus *Listonella* and reassignment of *Listonella damselae* (Love et al.) MacDonell and Colwell to the genus *Photobacterium* as *Photobacterium damselae* comb. nov. with an emended description. Int J Syst Bacteriol 1991;41:529–34.
[5] Okuzumi M, Okuda S, Awano S. Isolation of psychrophilic and halophilic histamine-forming bacteria from *Scomber japonicus*. Bull Jpn Soc Sci Fish 1981;47: 1591–8.
[6] Yoguchi R, Okuzumi M, Fujii T. Seasonal variation in numbers of mesophilic and halophilic histamine-forming bacteria in inshore of Tokyo Bay and Sagami Bay. Nippon Suisan Gakkaishi 1990;56:1467–72. In Japanese.
[7] Yoguchi R, Okuzumi M, Fujii T. Seasonal variation in numbers of mesophilic and halophilic histamine-forming bacteria on marine fish. Nippon Suisan Gakkaishi 1990;56:1473–9. In Japanese.

[8] Okuzumi M, Hiraishi A, Kobayashi T, Fujii T. *Photobacterium histaminum* sp. nov., a histamine-producing marine bacterium. Int J Syst Bacteriol 1994;44:631–6.
[9] Kimura B, Hokimoto S, Takahashi H, Fujii T. *Photobacterium histaminum* Okuzumi et al. 1994 is a later subjective synonym of *Photobacterium damselae* subsp. *damselae* (Love et al. 1981) Smith et al. 1991. Int J Syst Evol Microbiol 2000;50:1339–42.
[10] Janssen WA, Surgalla MJ. Morphology, physiology, and serology of a *Pasteurella* species pathogenic for white perch (*Roccus americanus*). J Bacteriol 1968;96: 1606–10.
[11] Gauthier G, Lafay B, Ruimy R, Breittmayer V, Nicolas JL, Gauthier M, et al. Small-subunit rRNA sequences and whole DNA relatedness concur for the reassignment of *Pasteurella piscicida* (Sniezko et al.) Janssen and Surgalla to the genus *Photobacterium* as *Photobacterium damselae* subsp. *piscicida* comb. nov. Int J Syst Bacteriol 1995;45:139–44.
[12] Thyssen A, Grisez L, van Houdt R, Ollevier F. Phenotypic characterization of the marine pathogen *Photobacterium damselae* subsp. *piscicida*. Int J Syst Bacteriol 1998;48:1145–51.
[13] Botella S, Pujalte MJM, Macián C, Ferrús MA, Hernández J, Garay E. Amplified fragment length polymorphism (AFLP) and biochemical typing of *Photobacterium damselae* subsp. *damselae*. J Appl Micobiol 2002;93:681–8.
[14] Fouz B, Larsen JL, Nielsen B, Barja JL, Toranzo AE. Characterization of *Vibrio damsela* strains isolated from turbot *Scophthalmus maximus* in Spain. Dis Aquat Org 1992;12:155–66.
[15] Grimes DJ, Stemmler J, Hada H, May EB, Maneval D, Hetrick FM, et al. *Vibrio* species associated with mortality of sharks held in captivity. Microb Ecol 1984; 10:2271–82.
[16] Pedersen K, Dalsgaard I, Larsen L. *Vibrio damsela* associated with diseased fish in Denmark. Appl Environ Microbiol 1997;63:3711–5.
[17] Fujioka RS, Greco SB, Cates MB, Schroeder JP. *Vibrio damselae* from wounds in bottlenose dolphins, *Tursiops truncatus*. Dis Aquat Org 1988;4:1–8.
[18] Clarridge JE, Zighelboim-Daum S. Isolation and characterization of two hemolytic phenotypes of *Vibrio damsela* associated with a fatal wound infection. J Clin Microbiol 1985;21:302–6.
[19] Fraser SL, Purcell BK, Delgado Jr B, Baker AE, Whelen AC. Rapidly fatal infection due to *Photobacterium (Vibrio) damsela*. Clin Infect Dis 1997;25:935–6.
[20] Lang M. Fatal *Vibrio damsela* bacteremia. Clin Microbiol Newslett 1992;14: 166–7.
[21] Perez-Tirse J, Levine JF, Mecca M. *Vibrio damsela*: a cause of fulminant septicemia. Arch Intern Med 1993;153:1838–40.
[22] Shin JH, Shin HG, Suh SP, Ryang DW, Rew JS, Nolte FS. Primary *Vibrio damsela* septicemia. Clin Infect Dis 1996;22:856–7.
[23] Yamane K, Asato J, Kawade N, Takahashi H, Kimura B, Arakawa Y. Two cases of fatal necrotizing fasciitis caused by *Photobacterium damsela* in Japan. J Clin Microbiol 2004;42:1370–2.
[24] Yuen KY, Ma L, Wong SSY, Ng WF. Fatal necrotizing fasciitis due to *Vibrio damsela*. Scand J Infect Dis 1993;25:659–61.
[25] Okuzumi M. Psychrophilic histamine-forming bacteria on/in marine fish. J Jpn Soc Cold Pres Food 1993;19:30–40.
[26] Buck JD. Potentially pathogenic marine *Vibrio* species in seawater and marine animals in the Sarasota, Florida, area. J Coastal Res 1990;6:943–8.
[27] Ghinsberg RC, Drasinover V, Sheinberg Y, Nitzan Y. Seasonal distribution of *Aeromonas hydrophila* and *Vibrio* species in Mediterranean coastal water and beaches: a possible health hazard. Biomed Lett 1995;51:151–9.
[28] Fouz B, Barja JL, Amaro C, Rivas C, Toranzo AE. Toxicity of the extracellular products of *Vibrio damsela* isolated from diseased fish. Curr Microbiol 1993;27: 341–7.
[29] Roux FL, Goubet A, Thompson FL, Faury N, Gay M, Swings J, et al. *Vibrio gigantis* sp. nov., isolated from the haemolymph of cultured oysters (*Crassostrea gigas*). Int J Syst Evol Microbiol 2005;55:2251–5.
[30] Franco PF, Hedreyda CT. Amplification and sequence analysis of the full length toxR gene in *Vibrio harveyi*. J Gen Appl Microbiol 2006;5:281–7.
[31] Bisharat N, Amaro C, Fouz B, Llorens A, Cohen DI. Serological and molecular characteristics of *Vibrio vulnificus* biotype 3: evidence for high clonality. Microbiology 2007;153:847–56.
[32] Takahashi H, Sato M, Kimura B, Ishikawa T, Fujii T. Evaluation of PCR-single strand conformational polymorphism analysis for identification of gram-negative histamine-producing bacteria isolated from fish. J Food Prot 2007;70: 1200–5.
[33] Osorio CR, Collins MD, Romalde JL, Toranzo AE. Characterization of the 23S and 5S rRNA genes and 23S-5S intergenic spacer region (ITS-2) of *Photobacterium damselae*. Dis Aquat Org 2004;61:33–9.
[34] Yamamoto S, Harayama S. PCR amplification and direct sequencing of *gyrB* genes with universal primers and their application to the detection and taxonomic analysis of *Pseudomonas putida* strains. Appl Environ Microbiol 1995; 61:1104–9.
[35] Kreger AS. Cytolytic activity and virulence of *Vibrio damsela*. Infect Immun 1984;44:326–31.
[36] Kothary MH, Kreger AS. Purification and characterization of an extracellular cytolysin produced by *Vibrio damsela*. Infect Immun 1985;49:25–31.
[37] Osorio CR, Romalde JL, Barja JL, Toranzo AE. Presence of phospholipase-D (*dly*) gene coding for damselysin production is not a pre-requisite for pathogenicity in *Photobacterium damselae* subsp. *damselae*. Microb Pathog 2000;28:119–26.
[38] Thyssen A, van Eygen S, Hauben L, Goris J, Swings J, Ollevier F. Application of AFLP for taxonomic and epidemiological studies of *Photobacterium damselae* subsp. *piscicida*. Int J Syst Evol Microbiol 2000;50:1013–9.
[39] Takahashi H, Kimura B, Yoshikawa M, Fujii T. Cloning and sequencing of the histidine decarboxylase genes of gram-negative, histamine-producing bacteria and their application in detection and identification of these organisms in fish. Appl Environ Microbiol 2003;69:2568–79.
[40] Miyaki T. Scombroid fish poisoning. Food Sanit Res 1954;12:7–14.
[41] Niven CF, Jeffrey MB, Corlett DA. Differential plating medium for quantitative detection of histamine-producing bacteria. Appl Environ Microbiol 1981;41: 321–2.
[42] Lane DJ. 16S/23S rRNA sequencing. In: Stackebrandt E, Goodfellow M, editors. Nucleic acid techniques in bacterial systematics. Chichester, UK: Wiley & Sons; 1991. p. 115–75.
[43] Sambrook J, Fritsch EF, Maniatis T. Molecular cloning: a laboratory manual. 2nd ed. Cold Spring Harbor, NY: Cold Spring Harbor Laboratory Press; 1989.
[44] Reed LJ, Muench H. A simple method of estimating fifty percent endpoints. Am J Hyg 1938;27:493–7.

International Journal of Food Microbiology 124 (2008) 239–249

Contents lists available at ScienceDirect

International Journal of Food Microbiology

journal homepage: www.elsevier.com/locate/ijfoodmicro

Development of a multilocus variable-number of tandem repeat typing method for *Listeria monocytogenes* serotype 4b strains

Satoko Miya [a], Bon Kimura [a,*], Miki Sato [a], Hajime Takahashi [a], Tatsuya Ishikawa [a], Takayuki Suda [a], Chikako Takakura [a], Tateo Fujii [a], Martin Wiedmann [b]

[a] Department of Food Science and Technology, Faculty of Marine Science, Tokyo University of Marine Science and Technology, 4-5-7 Konan, Minato-ku, Tokyo 108-8477, Japan
[b] Department of Food Science, Cornell University, Ithaca, New York, United States

ARTICLE INFO

Article history:
Received 11 July 2007
Received in revised form 17 March 2008
Accepted 24 March 2008

Keywords:
Listeria monocytogenes
4b
Subtyping
Epidemic clones

ABSTRACT

Listeria monocytogenes serotype 4b strains have been identified as the causative agent in many human listeriosis epidemics as well as in a considerable number of sporadic cases. Due to the genetic homogeneity of serotype 4b isolates, development of rapid subtyping methods with high discriminatory power for serotype 4b isolates is required to allow for improved outbreak detection and source tracking. In this study, multilocus variable-number tandem repeat analysis (MLVA) was developed and used to characterize 60 serotype 4b isolates from various sources. All isolates were also characterized by automated EcoRI ribotyping, single enzyme pulsed-field gel electrophoresis (PFGE) with ApaI, and a multilocus sequence typing (MLST) scheme targeting six virulence and virulence-associated genes. Discriminatory power of MLVA (as determined by Simpson Index of Discrimination) was higher than the discriminatory power of any of the other three methods. MLVA markers targeted were found to be stable and did not change when three isolates were passaged daily for 70 days. Cluster analyses of MLVA, PFGE and MLST consistently grouped the same isolates into three major clusters, each of which includes one of the three major *L. monocytogenes* epidemic clones (i.e., ECI, ECIa and ECII). We conclude that the MLVA method described here (i) provides for more discriminatory subtyping of *L. monocytogenes* serotype 4b strains than the other three methods, (ii) identifies three major groups within the serotype 4b, which are consistent with the groups identified by other subtyping methods, and (iii) is easy to interpret. Use of MLVA may thus be recommended for subtyping of serotype 4b isolates, including as a secondary more discriminatory subtyping method that could be used after initial isolate characterization by PFGE or ribotyping.

1. Introduction

Listeria monocytogenes is an ubiquitous bacterium that can cause severe invasive foodborne disease in humans. While 13 different serotypes have been identified in this organism to date, serotype 4b isolates have been responsible for most human listeriosis epidemics and are responsibly for the majority of human sporadic cases in many parts of the world (Farber and Peterkin, 1991; Schuchat et al., 1991). Serotype 4b isolates have been reported to be highly clonal and are genetically more homogeneous than other common *L. monocytogenes* serotypes (Graves et al., 1994; Mereghetti et al., 2002; O'Donoghue et al., 1995; Ridley, 1995). Specific highly clonal serotype 4b strains that have been responsible for multiple human listeriosis outbreaks have been classified into specific epidemic clones (EC), including ECI, ECIa (Kathariou, 2003), and ECII (Evans et al., 2004). The vast majority of *L. monocytogenes* serotype 4b isolates group into lineage I, which is predominant among human clinical listeriosis cases. In addition, a few atypical and genetically distinct serotype 4b isolates group into *L. monocytogenes* lineage III; while only lineage I serotype 4b strain are the focus of the study reported here, two lineage III serotype 4b isolates were also initially characterized by the MLVA method reported here.

Considering the highly clonal nature and genetic homogeneity of lineage I serotype 4b strains as well as their common involvements in human listeriosis cases and outbreaks, it is critical to develop rapid molecular subtyping methods that provide increased discrimination of these strains over existing subtyping methods. A number of molecular subtyping methods have been developed for and are commonly used for *L. monocytogenes*, including automated ribotyping, pulsed-field gel electrophoresis (PFGE), and more recently different multilocus sequence typing procedures targeting housekeeping as well as virulence genes (e.g., Cai et al., 2002; Revazishvili et al., 2004; Salcedo et al., 2003; Zhang et al., 2004; reviewed by Wiedmann, 2002). Automated ribotyping represents a highly reproducible and standardized subtyping method, which appears to be able to classify serotype 4b strains into epidemic clones as ECI and ECIa strains appear to be represented by ribotypes DUP-1038 and DUP-1042, respectively

* Corresponding author. Tel./fax: +81 3 5463 0603.
E-mail address: kimubo@kaiyodai.ac.jp (B. Kimura).

0168-1605/$ – see front matter © 2008 Elsevier B.V. All rights reserved.
doi:10.1016/j.ijfoodmicro.2008.03.023

Table 1
Subtypes and characteristics of *L. monocytogenes* isolates used in this study

Isolate no.[a]	Origin	Isolation date (day/mo/yr)[c]	MLVA cluster	MLVA type (no. of repeats) for			Ribotype	MLST type[d]	PFGE type
				TR1	TR2	TR3			
Outbreak related isolates (4b)									
CIP103322[†]	Human (Switzerland, 1983–87)	1987	1	22	17	9	1038B	1	6
FSL J1-003[†]	Human (Nova Scotia, 1981)	1981	1	19	17	9	1038B	1**	2
FSL J1-220[†]	Human (Boston; 1979)	1979	3	23	12	7	1042B	9**	24
FSL N1-225	Human (US; 1998–99)	1998	2B	23	22	5	1044A	17*	16
CIP103575[†]	Food (milk, Massachusetts, 1983)	1983	3	24	12	7	1042B	12	22
FSL J1-116[†]	Human (United Kingdom, 1983–87)	1988	3	23	12	7	1042B	9**	22
FSL N3-013	Food (pate; United Kingdom, 1983–87)	1988	3	12	12	7	1042B	9**	22
FSL J1-119	Human (Los Angeles, 1985)	1985	1	12	17	9	1038B	1**	6
FSL J1-110[†]	Food (Los Angeles, 1985)	1985	1	12	17	9	1038B	1**	6
Other isolates (4b)									
ATCC19115[†]	Human	N/A	3	25	12	7	1042B	9	25
CIP101821[†]	Human	1985	3	14	12	6	1042B	11	27
CIP102551[†]	Human	1986	1	23	16	9	1038B	7	6
NCTC4885[†]	Human	1936	1	18	17	9	1038B	6	7
NCTC9863[†]	Human	1956	3	23	12	7	1042B	9	23
NCTC10527[†]	Human	1967	3	25	12	7	1042B	9	26
FSL C1-132	Human sporadic	14-Sep-98	1	18	17	9	1038A	1	1
FSL C1-134	Human sporadic	15-Oct-98	1	21	17	9	1038B	1	3
FSL F2-021	Human sporadic	27-Jul-99	1	14	19	9	1038B	1	6
FSL F2-022	Human sporadic	3-Aug-99	2A	15	17	5	1042B	19	10
FSL F2-024	Human sporadic	4-Aug-99	2B	23	18	5	1044A	17	17
FSL F2-037	Human sporadic	23-Sep-99	1	14	19	9	1038B	1	6
FSL F2-091	Human sporadic	3-Aug-99	3	14	12	6	1042B	9	27
FSL F2-140	Human sporadic	14-Sep-99	2A	15	14	5	116-363-S-2	21	13
FSL F2-243	Human sporadic	6-Jan-00	1	14	19	9	1038B	1	6
FSL F2-372	Human sporadic	26-May-00	1	14	19	9	1038B	1	6
FSL F2-382	Human sporadic	22-Mar-00	1	13	17	9	1038B	1	5
FSL F2-420	Human sporadic	16-Jun-00	2B	14	10	5	1044A	17	16
FSL F2-427	Human sporadic	20-Jul-00	2B	23	18	5	1044A	18	17
FSL F2-475	Human sporadic	5-Aug-00	2A	16	17	5	1042B	20	12
FSL F2-480	Human sporadic	23-Aug-00	1	11	17	9	1038B	8	6
FSL F2-601	Human	2001	2A	10	17	5	1042B	25	10
FSL F2-637	Human sporadic	14-May-01	2B	23	18	5	1044A	17	14
FSL F2-642	Human sporadic	29-May-01	2A	16	17	5	1042B	20	12
FSL F2-656	Human sporadic	4-Jul-01	3	26	12	7	1042A	9	25
FSL F2-658	Human	2001	1	26	17	9	1038B	1	4
FSL F2-661	Human sporadic	20-Apr-01	3	27	12	7	1042B	9	27
FSL F2-672	Human sporadic	31-Aug-01	2B	19	21	5	1044A	17	16
FSL F2-689	Human sporadic	2001	1	9	17	9	1027C	1	6
FSL M2-042	Human sporadic	16-Feb-99	3	16	12	7	1042B	10	23
FSL J1-012[†]	Human	N/A	1	16	17	9	1038B	1	7
NCTC11994[†]	Food (soft cheese, assoc. with human case)	1986	1	18	17	9	1038B	3	8
ATCC51777[†]	Food (cheese)	N/A	1	18	17	9	1038B	2	8
20-5-1[†]	Food (cod roe)	28-Oct-04	2A	15	15	5	1042A	23	20
34-18-2[†]	Food (cod roe)	28-Apr-05	2A	16	15	5	1042A	16	21
Lma5[†]	Food (pork); plant A	N/A	2B	14	21	5	1044A	17	15
Lma7[†]	Food (pork); plant A	N/A	2B	14	21	5	1044A	17	14
Lmb15[†]	Food (pork); plant B	28-May-90	2A	11	15	5	1042A	15	19
Lmb17[†]	Food (pork); plant B	28-May-90	2A	11	15	5	1042A	14	18
Lmb20[†]	Food (pork); plant B	3-Jun-90	2B	22	21	5	1044A	17	14
Lmc1[†]	Food (pork), plant F	N/A	3	25	12	7	172-75-S-1	13	27
Lmc26[†]	Food (pork), plant C	N/A	3	15	12	7	1042B	9	27
Lmc32[†]	Food (pork), plant G	N/A	3	14	12	7	1042A	9	27
Lmc39[†]	Food (pork), plant F	N/A	3	25	12	7	172-75-S-1	9	27
FSL F2-001	Food (fresh white cheese)	28-Jun-99	2B	14	10	5	1044A	17	16
FSL F2-281	Food (white fish salad)	3-Feb-00	1	26	17	9	1027B	5	9
FSL E1-055	Animal (bovine)	1999	1	19	17	9	1038B	1	6
FSL E1-124	Animal (bovine)	1-Jun-01	1	19	17	9	1038B	4	6
FSL E1-125	Animal (caprine)	12-Jun-01	2A	15	14	5	1042B	22	12
FSL J2-039	Animal (wild turkey)	1993	2A	10	8	5	1042B	24*	11
FSL N4-289	Animal	2001	1	15	19	9	1038B	1	6
FSL F2-525[b]	Human sporadic (lineage III)	30-Aug-00	N/A	N/A[e]	14	N/A	1061A	26	28
FSL J1-158[b]	Animal (caprine) (lineage III)	Jul-97	N/A	N/A	14	N/A	10142	27	29
Other isolates (1/2a, 1/2b)									
FSL C1-117 (1/2a)	Human sporadic	9-Oct-98	N/A	16	16	9	1039C	28	30
FSL F2-029 (1/2a)	Human sporadic	29-Aug-99	N/A	8	13	9	1062D	34	31
FSL F2-048 (1/2a)	Human sporadic	24-Sep-99	N/A	21	18	9	1053A	32	32
39-17-1 (1/2a)	Food (salmon roe)	21-Jul-05	N/A	16	11	9	1030A	33	33
FSL E1-042 (1/2a)	Animal (bovine)	Apr-00	N/A	16	11	9	1030A	33	33
FSL E1-123 (1/2a)	Animal (bovine)	22-Jun-01	N/A	20	15	9	1039C	35	34

Table 1 (*continued*)

Isolate no.[a]	Origin	Isolation date (day/mo/yr)[c]	MLVA cluster	MLVA type (no. of repeats) for			Ribotype	MLST type[d]	PFGE type
				TR1	TR2	TR3			
Other isolates (1/2a, 1/2b)									
FSL F2-026 (1/2b)	Human sporadic	29-Jun-99	N/A	21	18	9	1043A	30	35
FSL F2-245 (1/2b)	Human sporadic	20-Jan-00	N/A	8	13	9	1052A	30	35
29-10-1 (1/2b)	Food (minced tuna)	17-Feb-05	N/A	14	15	6	1051D	31	36
FSL E1-039 (1/2b)	Animal (bovine)	Apr-00	N/A	16	16	9	1042B	36	37
FSL E1-041 (1/2b)	Animal (ovine)	Apr-00	N/A	16	11	9	1042C	29	38
FSL E1-058 (1/2b)	Animal (bovine)	May-00	N/A	20	15	9	1028A	30	39

[a] Isolates marked with a † were used for initial MLVA.
[b] Isolates FSL F2-525 and FSL J1-158 represent lineage III serotype 4b isolates.
[c] Isolation year, month, or date are given where available.
[d] For MLST types marked with a * and ** MLST data were obtained from a previous publication (Zhang et al., 2004 and Chen et al., 2007, respectively); for all other isolates MLST types were determined as part of the study reported here.
[e] N/A = not applicable; the lineage III serotype 4b strains did not have clear tandem repeat sequences in the TR1 and 3 amplicons.

(Jeffers et al., 2001), while ECII is represented by ribotype DUP-1044A (Gray et al., 2004). However, ribotyping has lower discriminatory power than PFGE for *L. monocytogenes*, in particular for serotype 4b strains (Aarnisalo et al., 2003; Grif et al., 2006). PFGE, on the other hand, generally provides for highly discriminatory subtyping of *L. monocytogenes* and is often considered the gold standard subtyping method for this organism. However, even with the standard PulseNet two-enzyme PFGE protocol, the ability to discriminate serotype 4b isolates and epidemic clones may be limited. For example, a recent study found that 15 ribotype DUP-1038B isolates from human cases, foods, animals and environmental sources in New York State as well as isolates from the 1985 listeriosis outbreak in Los Angeles and from the 1983–87 outbreak in Switzerland all shared the same PFGE type (Fugett et al., 2007). In addition, fragment-based methods like PFGE may be difficult to standardize and compare between laboratories and PFGE data do not allow for phylogenetic analyses (Wiedmann, 2002). MLST methods overcome many of the limitations of PFGE (Maiden et al., 1998), but MLST also only allows for limited discrimination of serotype 4b isolates and epidemic clones (Borucki et al., 2004; Zhang et al., 2004). For example, the MLST protocol established by Zhang et al. (2004) was not able to differentiate ECII isolates linked to two different outbreaks in the US (Chen et al., 2007), even though isolates from these outbreaks could be differentiated by PFGE (Chen et al., 2005).

Analysis of tandem repeat sequences has been utilized for molecular subtyping since there are potentially extensive polymorphisms in the number of repeats among individuals of the same species (Schlötterer and Tautz, 1992) or clonal group. A subtyping approach that targets multiple variable-number of tandem repeat (VNTR) loci, often called multiple-locus VNTR analysis (MLVA), has been used successfully for discriminatory subtyping of a number of bacterial pathogens, including *Bacillus anthracis* (Keim et al., 2000; Le Flèche et al., 2001; Ryu et al., 2005), *Escherichia coli* (Lindstedt et al., 2004a; Noller et al., 2003), *Haemophilus influenzae* (van Belkum et al., 1997), *Mycobacterium tuberculosis* (Fronthingham and Meeker-O'Connell, 1998), *Neisseria meningitides* (Yazdankhah et al., 2005), *Salmonella enterica* (Lindstedt et al., 2004b; Ramisse et al., 2004), and *Yersinia pestis* (Klevytska et al., 2001). As MLVA has been shown to allow for sensitive subtype discrimination of highly clonal pathogens difficult to differentiate by other methods (e.g., *B. anthracis*, *Y. pestis*), we developed and validated a MLVA method to specifically discriminate *L. monocytogenes* serotype 4b strains and clonal groups. The MLVA method described here is easy to interpret and allows for rapid and sensitive subtyping of serotype 4b strains, using only 3 tandem repeat regions. The study reported here provides important data beyond those presented in a recent publication (Murphy et al., 2007), which investigated agarose gel-based MLVA for subtyping of *L. monocytogenes* using only food isolates, most of them representing serotype 1/2a.

2. Materials and methods

2.1. Bacterial isolates

A total of 60 *L. monocytogenes* lineage I, serotype 4b isolates were used in this study (Table 1). In addition to 39 isolates from the Cornell Food Safety Laboratory (FSL) collection, isolates were purchased from American Type Culture Collection (ATCC; Manassas, Va.), National Collection of Type Cultures (NCTC; London, United Kingdom), and Collection de l'Institut Pasteur (CIP; Paris, France). Two seafood isolates (Handa et al., 2005) and nine pork isolates were obtained from food products sampled in Japan. In total, 38 human isolates, 17 food isolates and 5 animal isolates representing lineage I and serotype 4b were included in this study. In addition to these 60 isolates, 6 serotype 1/2a isolates, 6 serotype 1/2b isolates, and two serotype 4b lineage III isolates were also characterized by MLVA; serotype 4b isolates in this lineage are rare and distinct from serotype 4b lineage I isolates (Roberts et al., 2006; Ward et al., 2004).

2.2. MLVA

Among more than 100 potential VNTRs identified by the Tandem Repeat Finder program (http://tandem.bu.edu/trf/trf.html) (Benson, 1999) in the genome sequence for *L. monocytogenes* F2365 (GenBank accession No. AE017262) (Nelson et al., 2004), three VNTR regions (TR1 to TR3), which showed the highest levels of allelic variation in initial studies among 26 of the isolates studied, were selected as targets for the final MLVA scheme (Table 2). These 26 isolates were included in the 60 isolates used for the further study. The predicted ORF designations and their functions were obtained from The Institute for Genomic Research Comprehensive Microbial Resource website (http://www.tigr.org) (Peterson et al., 2001).

L. monocytogenes DNA for PCR amplification of TR1 to TR3 was prepared using a DNA extraction kit (Mag Extractor-Genome; Toyobo

Table 2
Characteristics of VNTR loci used for MLVA

TR	Repeat motif	No. of alleles	Diversity[a]	Location in F2365[b]	No. of repeats in F2365[b]
TR1	CCGGTAGAT	17	0.924	1150428–1150552	14
TR2	CATCGG	11	0.798	1849463–1849564	17
TR3	TCA	4	0.686	196959–196985	9

[a] Diversity (expressed as Simpson's Index of Discrimination) was calculated based on MLVA data for the 60 L. monocytogenes lineage I serotype 4b isolates characterized here.
[b] Location and No. of repeats are based on the genome sequence for L. monocytogenes isolate F2365.

Co. Ltd., Tokyo, Japan) (Takahashi et al., 2003). PCR was performed in 20-μl mixtures containing 10 mM Tris–HCl (pH 8.3), 50 mM KCl, 1.5 mM $MgCl_2$, 20 pmol of each primer, 0.2 mM of each dNTP, 10 ng of template DNA and 0.5 U of Takara Taq DNA polymerase (Takara Bio, Otsu, Japan) using a Gene Amp 9700 thermal cycler (Applied Biosystems, Foster City, Calif.). PCR primers (Table 3) were designed from sequences flanking the TR1 to TR3 regions. PCR conditions included an initial denaturation step (94 °C for 5 min), followed by 30 cycles at 94 °C for 30 s, 60 °C for 40 s, 72 °C for 1 min, and a final extension of 72 °C for 4 min. The PCR amplification products were sequenced on an ABI PRISM 310 genetic analyzer (Applied Biosystems) with the Big Dye terminator v.3.0 cycle sequencing kit (Applied Biosystems).

To facilitate rapid typing, fragment size analysis of the TR1 to TR3 PCR products was also performed. For this purpose, the TR1 to TR3 forward primers were labeled with 6-carboxy-4,7,2',4',5',7'-hexachlorofluorescein (HEX), 6-carboxy-4,7,2',7'-tetrachloro-fluorescein (TET) and 5-carboxyfluorescein (FAM), respectively (Table 3). PCR amplification for fragment size analysis was performed in a 10-μl mixture containing 10 mM Tris–HCl (pH 8.3), 50 mM KCl, 1.5 mM $MgCl_2$, 1 pmol of fluorescently labeled forward primer and non-labeled reverse primer, 0.2 mM of each dNTP, 5 ng of template DNA and 0.25 U of Takara Taq DNA polymerase. A 1-μl aliquot of each PCR product was mixed with 10 μl of Hi-Di formamide (Applied Biosystems) and 1 μl of GeneScan-500 ROX size standard (Applied Biosystems). Capillary electrophoresis of PCR products was performed on an ABI PRISM 310 Genetic Analyzer with POP4-polymer using the standard GeneScan module with filter set C. MLVA types were assigned to TR1 through TR3 based on the number of repeats present for a given TR, e.g., TR1 type 22 for isolate CIP 103322 (Table 1) indicates that 22 TR1 repeats were found in this isolate.

2.3. Stability of MLVA patterns

To test the stability of *L. monocytogenes* MLVA patterns, three epidemiologically distinct isolates (Lma5, CIP103322, and CIP103575; Table 1) were passaged daily for 70 days in BHI broth. MLVA was performed on isolates obtained after every 10th passage.

2.4. MLST

Since *L. monocytogenes* serotype 4b isolates are highly clonal, we used a MLST scheme previously described by Zhang et al. (2004), which is based on DNA sequencing of 6 *L. monocytogenes* virulence and virulence-associated genes, to further characterize all serotype 4b isolates that were characterized by MLVA. Zhang et al. (2004) referred to this approach as multi-virulence-locus sequence typing (MVLST). PCR amplification and DNA sequencing was performed essentially as described by Zhang et al. (2004); sequencing reactions were run using an ABI PRISM 310 Genetic Analyzer. For each locus, DNA sequences that differed by at least one nucleotide were assigned different arbitrary allele numbers (Maiden et al., 1998).

Table 3
PCR primers and amplification conditions for selected VNTR loci[a]

Locus	Primer	Sequence (5'–3')[b]	PCR products	
			Location in F2365	Length
TR1	TR-1f	HEX-ACATGGGAAGGGTTGCAA	1150293–1150591	299
	TR-1r	GGATTTACTTGATTTGACGGGT		
TR2	TR-2f	TET-CCATGGAAGACTACTGTTTGTA	1849739–1849272	468
	TR-2r	GACGGTACTGTTATCGGAAA		
TR3	TR-3f	FAM-GAAGGTAAAAACGGCGAAAAA	196776–197158	383
	TR-3r	ATTGCTTCTCCGTATCCCTCA		

[a] The primers outlined, synthesized without fluorescent dyes, here were also used for sequencing analysis.
[b] Primers were designed using the genome sequence for *L. monocytogenes* isolate F2365; HEX, TET, and FAM indicate the fluorescent dyes used to label a given primer.

2.5. PFGE

Single enzyme PFGE with ApaI, instead of the standard PulseNet two-enzyme PFGE protocol with ApaI and AscI, was performed as described by Graves and Swaminathan (2001) with minor modification. DNA plugs for PFGE were made using CHEF bacterial plug kit (Bio-Rad, Hercules, Calif.). Briefly, *L. monocytogenes* strains were grown overnight in BHI medium, followed by addition of chloramphenicol to a final concentration of 180 μg/ml and subsequent incubation for up to 1 h at 30 °C. Bacterial cells were then pelleted by centrifugation at 10,000 rpm for 5 min, resuspended in 100 μl of cell suspension buffer (10 mM Tris pH 7.2, 20 mM NaCl, 50 mM EDTA), and equilibrated to 50 °C. Bacterial suspensions were mixed with equal volumes of CleanCut agarose (2%, 50 °C) and poured into a mold to form agarose plugs (15 min, 4 °C). Plugs with immobilized bacteria were incubated for 2 h at 37 °C in a lysozyme solution, rinsed with sterile water, and subsequently incubated overnight at 50 °C in proteinase K solution. Plugs were then washed four times (1 h each) with 1 ml of 1 × wash buffer with gentle agitation at room temperature for 1 h, followed by overnight incubation with 30 U of ApaI (New England Biolabs, Beverly, MA) in 300 μl of 1 × enzyme buffer. Following the restriction digest, the plugs were incubated in 1 ml of 1 × wash buffer for 30 min with gentle agitation. One-third of each plug was placed in 1.0% agarose (Seakem Agarose Gold; FMC Bioproducts, Rockland, ME) gel in 0.5 × TBE buffer. PFGE was performed for 22 h at 14 °C with the CHEF-DR II system (Bio-Rad) at 6 V/cm with switch times ranging from 4 to 40 s. Gels were stained with ethidium bromide and photographed while transilluminated with UV light.

2.6. Ribotyping

Ribotyping data were already available for all isolates obtained from the Cornell strain collection (Table 1). For all other isolates, automated EcoRI ribotyping was carried out using the RiboPrinter microbial characterization system (Qualicon Inc., Wilmington, Del.) according to manufacturer's instructions, using isolates grown overnight at 30 °C on BHI agar plates; this represents the same procedure that was used to characterize all isolates obtained from Cornell. The RiboPrinter instrument automatically performs cell lysis and restriction enzyme digestion followed by gel electrophoresis and Southern hybridization with an rRNA gene probe. Images are analyzed using the RiboPrinter analysis software, which normalizes fragment pattern data for band intensity and band size relative to molecular weight markers. Patterns were then compared to the RiboPrinter database for characterization; a DuPont ID (e.g., DUP-1038) is automatically assigned to a ribotype pattern that matches a DuPont ID pattern with a similarity of 0.85 or above. If visual inspection observed more than one distinct ribotype pattern within a given Dupont ID, an alphabetical letter was assigned at the end of each Dupont ID (e.g. DUP-1038A, DUP-1038B); assignment of these refined IDs was performed by comparing ribotype patterns to patterns in the Cornell University PathogenTracker database (http://www.pathogentracker.net). If a given ribotype pattern did not match a DuPont ID pattern with a similarity > 0.85 (and thus was not assigned a DuPont ID), we assigned a unique type designation based on the "Ribogroup" that had been assigned by the instrument (e.g., ribogroup 172-75-S-1) after visual inspection and confirmation.

2.7. Data analysis

MLVA and MLST data (i.e., numerical types for TR1 to 3 [representing the number of repeats in a given TR] and MVLST allelic types for all 6 genes) were analyzed using the BioNumerics v.4.0 software (Applied Maths, Sint-Martens-Latem, Belgium). Cluster analysis using the numerical profiles for each isolate was performed using the categorical coefficient and the UPGMA method. For PFGE, gel

images in TIFF format were processed with BioNumerics software; cluster analysis was performed by UPGMA using Dice coefficient with 1.5% tolerance (Graves and Swaminathan, 2001).

2.8. Discriminatory index (DI)

Discriminatory power, i.e., the ability to distinguish between unrelated strains, was calculated using Simpson's index of diversity (DI, Hunter and Gaston, 1988). As the value approaches 1, the power of the method to discriminate unrelated strains increases. For MLVA, DI was calculated separately for each TR region as well as based on the combined MLVA type, which considered that data for all three TR regions.

3. Results

3.1. VNTR profiles

Among more than 100 potential TRs initially identified in the genome of *L. monocytogenes* F2365, seven were selected for initial analysis using a set of 26 isolates. Subsequently, three repeat regions, which were found to be highly variable and could consistently be amplified in all serotype 4b isolates tested, were selected for analysis in 60 serotype 4b isolates, including the initial 26 isolates (Table 1). All three VNTR regions are located within ORFs, including two ORFs encoding surface anchored cell wall proteins (TR1 and TR2; TIGR annotation 1144 and 1826, respectively), and one ORF encoding a conserved hypothetical protein (TR3; TIGR annotation 0197). DNA sequencing of the PCR products for TR1 to TR3 identified 17, 11, and 4 alleles of different lengths for TR1, TR2, and TR3, respectively (Tables 1 and 2). When analyzed separately, TR1 showed the highest discriminatory power (DI=0.924), followed by TR2 (DI=0.798) and TR3 (DI=0.686). The number of repeats for a given TR varied from 9 to 27 for TR1, 8 to 22 for TR2, and 5 to 9 for TR3 (Table 1). Although the numbers of nucleotides in each repeat unit were stable for each TR (9, 6 and 3 nucleotides in each repeat unit of TR1, 2 and 3, respectively), repeat sequences occasionally showed small variations within a given isolate. For example, in isolate FSL C1-132 most TR1 repeat units had a sequence of CCGGTAGAT, while some repeats represented sequence variants, such as CCGGTAGAC. TR 2 and 3 showed similar sequence variations among repeat sequences within a given isolate. When all three TR types were analyzed together a total of 37 MLVA types could be differentiated among the 60 serotype 4b isolates.

Since a sequencing based approach to characterization of VNTRs (as detailed in the previous paragraph) requires each TR region to be analyzed separately, we also developed and validated a capillary electrophoresis-based analysis approach that allows for all 3 VNTR loci to be characterized simultaneously. With this approach, electropherograms could be obtained within 30 min after completion of PCR amplification. For each isolate, three peaks (corresponding to TR1, 2, and 3) were clearly identifiable. However, the apparent sizes of the obtained fragments differed slightly from the sizes determined by DNA sequencing (i.e., up to 2 nt differences in TR1 and TR2, and 1 nt difference in TR3). These size differences may be due to secondary structure formation in the PCR products (Schouls et al., 2004). However, these discordances are small relative to the number of nucleotides in one repeat unit, and they thus do not affect the ability of capillary gel electrophoresis to accurately determine the repeat numbers in TR1 to TR3. Gel electrophoretic determination of TR repeat numbers was confirmed to be highly reproducible (i.e., each of the three runs yielded the same repeat numbers for all 60 serotype 4b isolates).

Some of the food isolates tested were obtained from the same plants. In three instances, isolates from the same plant had identical MLVA patterns, including (i) isolates Lma5 and Lma7 (plant A), these isolates showed identical MLST and ribotypes, but different PFGE patterns (Table 1); (ii) isolates Lmb15 and Lmb17 (plant B), these isolates showed identical ribotypes, but different PFGE types and MLST patterns (Table 1); and (iii) isolates Lmc1 and Lmc39 (plant F), these isolates showed identical PFGE types and ribotypes but different MLST patterns (Table 1).

3.2. Stability test of MLVA patterns

MLVA on three isolates that were passaged daily for 70 days and tested after each 10 passages showed no variation in repeat numbers for TR1, 2, or 3.

3.3. MLVA of selected L. monocytogenes isolates representing serotypes and lineage other than lineage I serotype 4b

Whereas TR2 and 3 were amplified successfully in6 serotype 1/2a and 6 serotype 1/2b isolates, no PCR product was initially obtained for these isolates for TR1 (Table 3). When primers targeting TR1 that had been reported by Murphy et al. (2007) were used on these 12 isolates, successful amplification of TR1 was obtained though. However, the lengths of the regions flanking TR1 in these isolates were different from the length of the TR1 flanking regions in isolates of serotype 4b, making it difficult to identify the repeat number for the serotype 1/2a and 1/2b isolates based on fragment size analysis. Thus, the TR1 region does not appear to be an appropriate for MLVA of *L. monocytogenes* isolates of different serotypes when fragment sizing is used to identify the number of repeats.

In addition, we also tested two serotype 4b isolates that grouped into *L. monocytogenes* lineage III. These two lineage III isolates showed 14 repeats in TR2 (Table 1), but did not have clear tandem repeat sequences in the TR1 and 3 amplicons, supporting the previous observations that lineage III serotype 4b strains are genetically distinct from lineage I serotype 4b strains and have a number of unique genetic characteristics (Liu et al., 2006; Roberts et al., 2006).

3.4. Ribotyping

The 60 serotype 4b isolates characterized by MLVA represented ribotypes DUP-1038B ($n=20$), DUP-1042B ($n=18$), DUP-1044A ($n=10$), and DUP-1042A ($n=6$) as well as five ribotypes that occurred only once or twice (Table 1).

3.5. PFGE

Single enzyme ApaI PFGE discriminated 27 subtypes among the 60 serotype 4b isolates. Isolates from a given outbreak showed the identical PFGE types, including FSL J1-119 and FSL J1-110 (representing isolates from the 1985 listeriosis outbreak in Los Angeles; Table 1) as well as isolates FSL J1-116 and FSL N3-013 (representing an isolate from the 1988–90 outbreak in the United Kingdom). Both of these isolate pairs also showed identical MLST types (Chen et al., 2007 Table 1). While the two isolates from the outbreak in the United Kingdom showed different MLVA types, the two isolates from the Los Angeles outbreak showed the same MLVA types.

3.6. Discriminatory ability of MLVA, PFGE, MLST, and ribotyping

MLVA, single enzyme PFGE, MLST, and ribotyping discriminated the 60 serotype 4b isolates tested into 37, 27, 25, and 9 different subtypes. Calculation of Simpson index for discrimination also showed that MLVA is more discriminatory (DI=0.980) than PFGE (DI=0.932), MLST (DI=0.874), and ribotyping (DI=0.760). Even when the 26 isolates that were used for initial MLVA analysis set were excluded in DI value calculation (yielding only 34 isolates), the DI value for MLVA (0.957) was still higher than the DI values for PFGE (DI=0.898), MLST (DI=0.843), and ribotyping (DI=0.765). The improved discriminatory power of MLVA is also illustrated by the observation that ten isolates that all showed the same MLST and PFGE

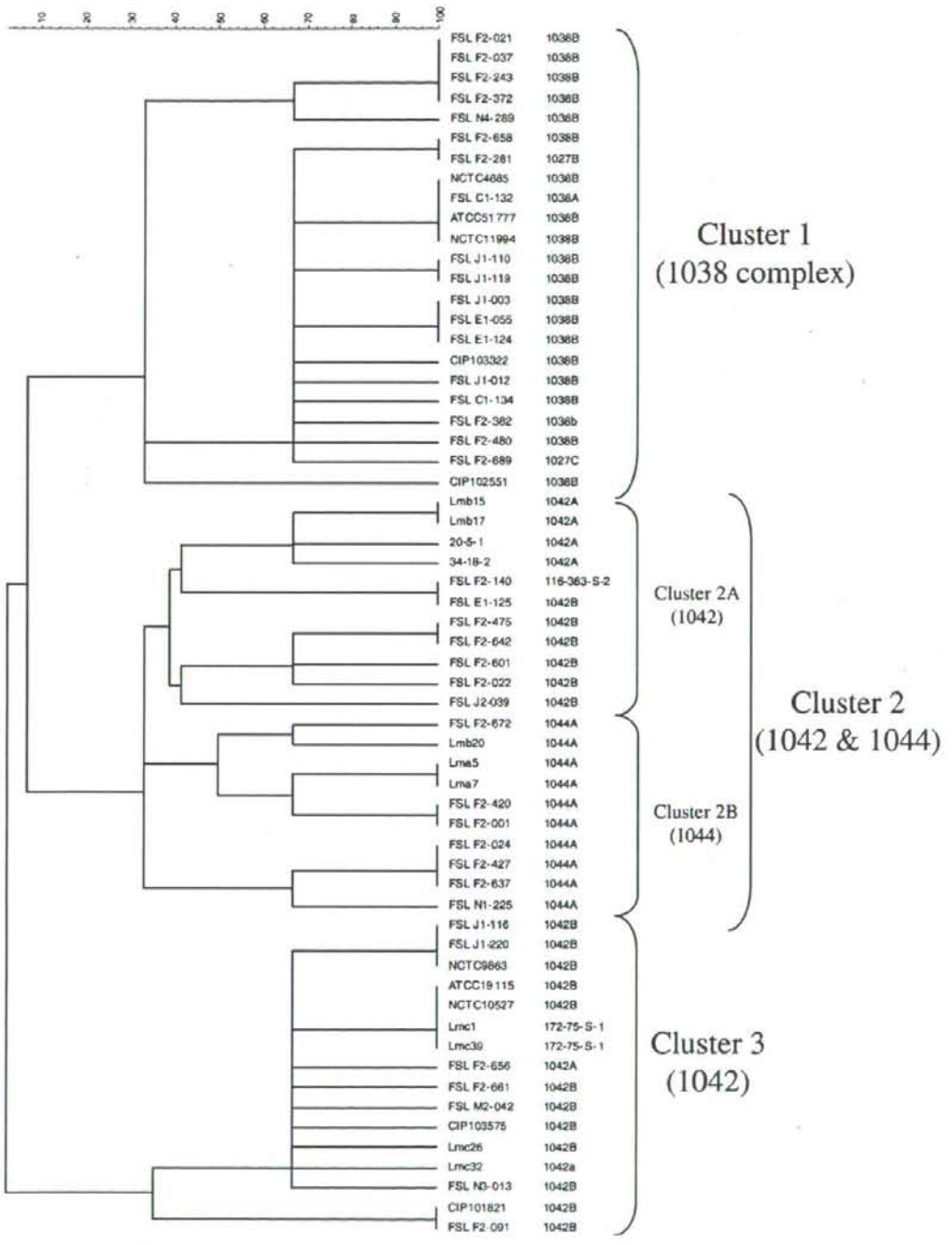

Fig. 1. MLVA-based dendrogram for 60 *L. monocytogenes* serotype 4b isolates. The dendrogram was constructed based on repeat numbers for TR1, 2, and 3 (as determined by DNA sequencing) using the categorical coefficient and the UPGMA method. Similarity percentages are shown above the dendrogram (extremely low similarities occur because some isolates may differ in repeat numbers for all three TRs). A dendrogram constructed based on fragment size obtained by capillary electrophoresis would be identical since the same allelic variants were defined by this method. The tree displayed is a dendrogram based on fragment size data and cannot be construed as a phylogenetic tree.

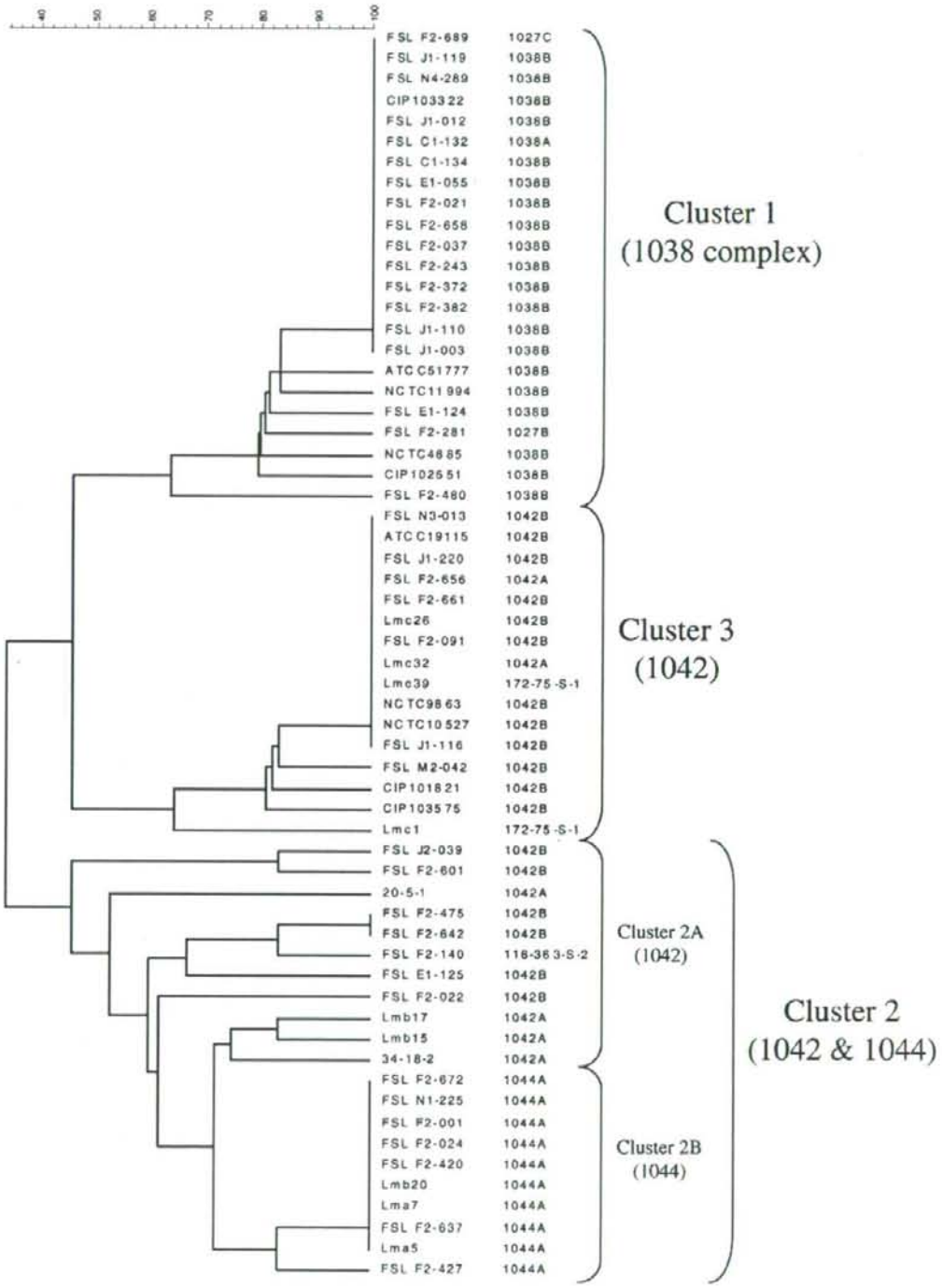

Fig. 2. MLST-based dendrogram for 60 *L. monocytogenes* serotype 4b isolates. The dendrogram was constructed based on allelic types for the 6 genes sequenced using the categorical coefficient and the UPGMA method.

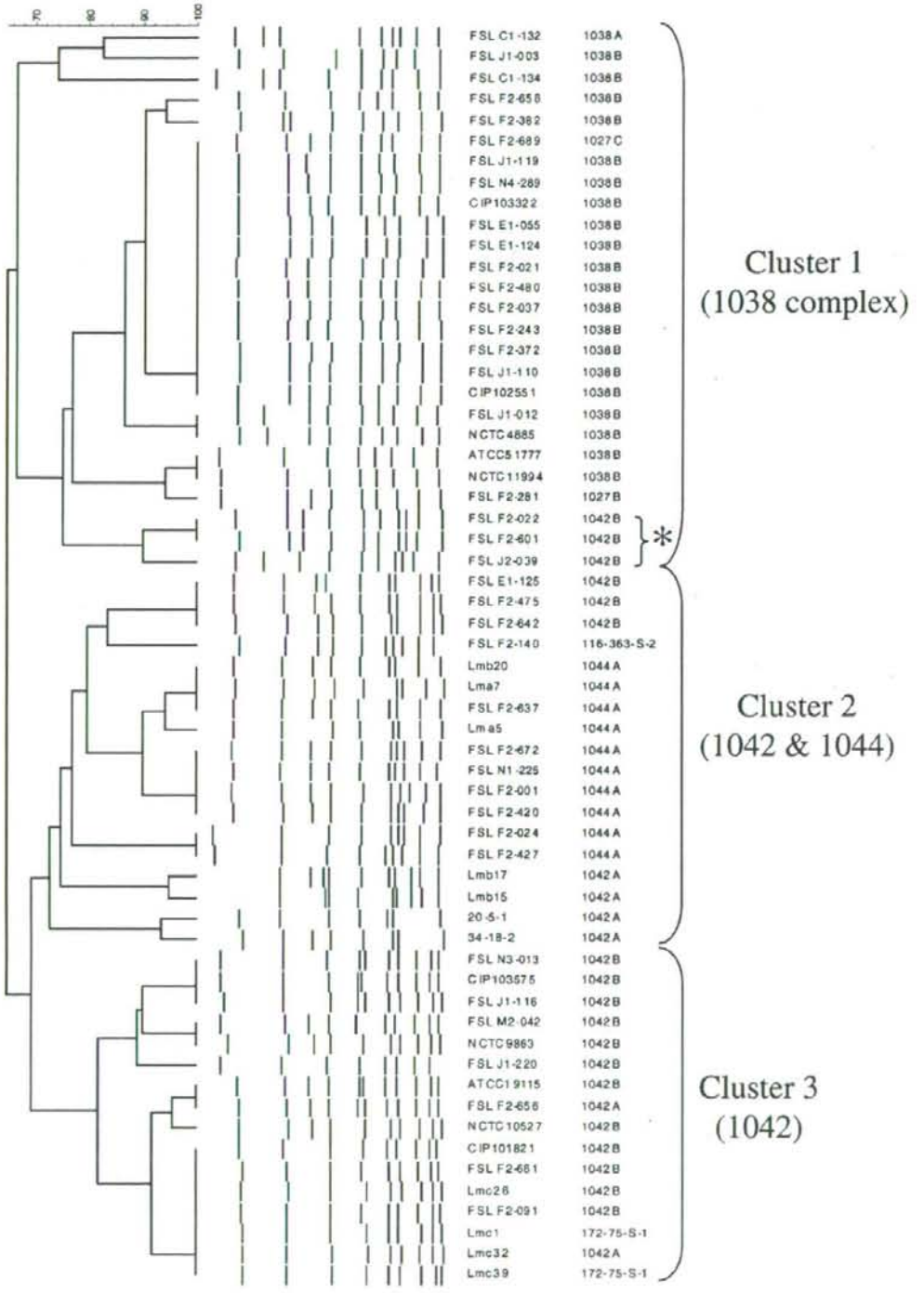

Fig. 3. ApaI PFGE-based dendrogram for 60 *L. monocytogenes* serotype 4b isolates. The dendrogram was constructed using the Dice coefficient and UPGMA method. Band positions were assigned using the BioNumerics software. The three isolates marked by an asterisk represent ribotype DUP-1042B isolates that clustered different based on PFGE types as compared to clustering based on MLVA and MLST types.

types (i.e., MLST type 1 and PFGE type 6; see Table 1), represented 6 different MLVA types; MLVA also differentiated two animal isolates from the human isolates in this group, indicating the ability of this MLVA protocol to differentiate apparently unrelated isolates that group together by PFGE and MLST.

3.7. Cluster analysis of MLVA, MLST, and PFGE patterns

A MLVA dendrogram constructed based on repeat number variation observed by sequence analysis (Fig. 1) yielded three major clusters that correlated well with ribotype as well as epidemic clone assignments of isolates. Cluster 1 included all isolates classified as ribotypes DUP-1038A, DUP-1038B, and DUP-1027. All isolates in this cluster had nine TR3 repeats, while none of the isolates in clusters 2 or 3 had nine TR3 repeats. All 4 ECI isolates included in the isolate set tested here (i.e., FSL J1-003, CIP103322, FSL J1-110 and FSL J1-119) grouped into cluster 1; these isolates represent the strains linked to the human listeriosis outbreaks from Nova Scotia (1981), Switzerland (1983–87), and Los Angeles (1985). Cluster 2 included isolates with DUP-1042B ($n=6$), DUP-1042A ($n=4$; all representing one cluster within cluster 2), as well as all the isolates classified as DUP-1044A. One isolate with a unique ribotype (FSL F2-140) also grouped into this cluster. Within cluster 2, isolates with ribotype DUP-1044A clustered separately from the isolates with other ribotypes. Cluster 2 included the ECII isolate FSL N1-225, a human isolate from the multistate human listeriosis outbreak that occurred in the US in 1998/99. All isolate in cluster 2 had five TR3 repeats, presence of 5 TR3 repeats was unique to isolates in this cluster.

Cluster 3 included isolates with ribotypes DUP-1042B (12 isolates), DUP-1042A (2 isolates), and 172-75-S-1 (2 isolates); all isolates in this cluster had 12 TR2 repeats. This cluster included the ECIa isolates FSL J1-116 and FSL N3-013 (isolates from the 1988–90 outbreak in the United Kingdom), FSL J1-220 (an isolate from the 1979 outbreak in Boston) and CIP103575 (an isolate from the 1983 outbreak in Massachusetts).

Cluster analysis based on MLST data yielded a dendrogram that provided very similar clustering to that observed in the MLVA dendrogram. The same three main clusters that were identified in the MLVA dendrogram were also observed in the MLST dendrogram (Fig. 2); grouping of isolates into these three clusters was the same for MLVA and MLST. Cluster analysis based on PFGE types (Fig. 3) also yielded essentially the same three clusters defined by MLVA and MLST. Grouping of isolates to clusters in the PFGE dendrogram was basically identical to the grouping found in MLVA and MLST dendrograms, with the exception of three ribotype DUP-1042 isolates, which were grouped into cluster 1 (which contained only DUP-1038B and DUP-1027 isolates in the MLVA and MLST dendrograms).

4. Discussion

We characterized 60 *L. monocytogenes* serotype 4b isolates, which represent a difficult to discriminate *L. monocytogenes* clonal group that is commonly involved in human listeriosis outbreaks and cases (Farber and Peterkin, 1991; Schuchat et al., 1991) using MLVA as well as MLST, PFGE, and ribotyping. Our data show that the MLVA method described here (i) provides for highly discriminatory subtyping of *L. monocytogenes* serotype 4b strains, (ii) identifies three major groups within the serotype 4b, which are consistent with the groups identified by other subtyping methods, and (iii) provides for rapid and reliable results when repeat variation is detected using a capillary electrophoresis-based approach.

4.1. MLVA provides for highly discriminatory subtyping of L. monocytogenes serotype 4b strains

Consistent with previous studies that have shown MLVA to be useful for typing closely related strains (Coletta-Filho et al., 2001; Keys et al., 2005; Klevytska et al., 2001), we have shown here that MLVA also provides for highly discriminatory subtyping of *L. monocytogenes* serotype 4b isolates. As MLVA targets highly variable genomic regions, concerns exist that MLVA markers may be unstable and may thus rapidly change during passage in the laboratory, natural environments, or infected hosts (van Belkum et al., 1998). This would potentially lead to different MLVA patterns for epidemiologically linked isolates, complicating surveillance and epidemiological investigations. To address this concern with the specific MLVA protocol developed here, lab passage experiments were performed, which showed that the MLVA markers used were stable during 70 passages in rich medium. While the serotype 4b isolate set used here generally represented unrelated isolates, we also included some epidemiologically related isolates in our study to initially evaluate the ability of the MLVA scheme described here to provide epidemiologically relevant subtype data. For example, human and food isolates from the 1985 listeriosis outbreak in Los Angeles showed the same MLVA type. Identical MLVA patterns were also found among food isolates obtained from each of three plants, providing initial support that MLVA can group together epidemiologically related food isolates; the fact that some of these isolates were differentiated by PFGE and/or the MLST protocol used here may even indicate that PFGE and MLST can sometimes detect differences that may not be epidemiologically relevant (i.e., epidemiologically related isolates may be grouped into different subtypes). In this context it is important to emphasize that our MLVA scheme targets ORFs, while PFGE can detect differences in *L. monocytogenes* prophage regions that can be highly variable and unstable, this possibly providing different subtypes for isolates from the same outbreak (Kathariou et al., 2006). Overall, our data indicate that MLVA generally groups epidemiologically related isolates into the same MLVA type, even though we identified one incidence (1983–87 human listeriosis outbreak in the United Kingdom) where epidemiologically linked human and food isolates represented different MLVA types (due to variation in one of the three TRs tested). As these food and human isolates represented an outbreak that occurred 20 years ago and as no information on the number of lab passages isolates were exposed to is available, it is possible that the MLVA (and MLST) differences between these isolates occurred during laboratory passages. Further MLVA studies using a larger set of, ideally low passage, epidemiologically related and unrelated serotype 4b isolates will be necessary to further define the likelihood that MLVA correctly classifies epidemiologically related and unrelated isolates into subtypes. In addition, MLVA of isolates passaged in animals may need to be performed to further assess the stability of the chosen markers, particularly since two of them are in surface molecules, which may be under selective pressure in an host, e.g., if they are targeted by host antibodies or cytotoxic T cells.

4.2. MLVA identifies three major groups within the serotype 4b, which are consistent with the groups identified by other subtyping methods

A considerable numbers of studies have indicated that *L. monocytogenes* strains differ in their virulence characteristics and/or in their associations with human listeriosis cases and outbreaks (Barbour et al., 2001; Franciosa et al., 2005; Jacquet et al., 2004; Olier et al., 2002; Roche et al., 2001). Consequently, a number of subtyping-based studies have classified *L. monocytogenes* into distinct lineages and clonal groups, including specific epidemic clones (Aarts et al., 1999; Brosch et al., 1994; Call et al., 2003; Ducey et al., 2007; Graves et al., 1994; Piffaretti et al., 1989; Rasmussen et al., 1995; Ward et al., 2004; Wiedmann et al., 1997). In general, most subtyping methods have identified two major, common *L. monocytogenes* lineages; one lineage contains the vast majority of serotype 1/2b and 4b isolates (classified as lineage I by some and division II by others [reviewed by Wiedmann, 2002]), while the other lineage contain predominantly serotype 1/2a and 1/2c isolates (Wiedmann, 2002). A third lineage, which is rarely